Journal Pre-proof

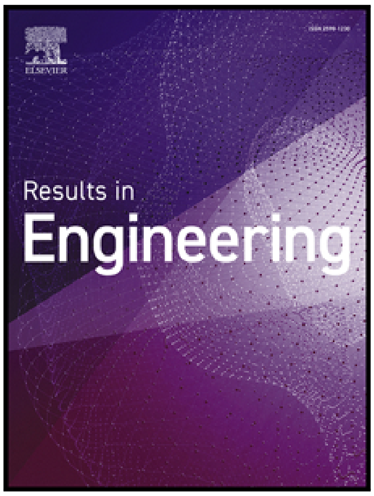

Thermo-Mechanical Performance and Techno-Economic Assessment of Lightweight Cement Mortar Incorporating a Coconut Shell Activated Carbon/PCM Composite for Thermal Energy Storage

M.F. Junaid , Z. ur Rehman , C. Fabiani , C. Chiatti , M. Matejdes , M. Slaný

PII: S2590-1230(26)03608-X
DOI: https://doi.org/10.1016/j.rineng.2026.112592
Reference: RINENG 112592

To appear in: *Results in Engineering*

Received date: 22 July 2026
Revised date: 11 August 2026
Accepted date: 21 August 2026

Please cite this article as: M.F. Junaid , Z. ur Rehman , C. Fabiani , C. Chiatti , M. Matejdes , M. Slaný , Thermo-Mechanical Performance and Techno-Economic Assessment of Lightweight Cement Mortar Incorporating a Coconut Shell Activated Carbon/PCM Composite for Thermal Energy Storage, *Results in Engineering* (2026), doi: https://doi.org/10.1016/j.rineng.2026.112592

Highlights

- Coconut shell activated carbon composite Bio PCM enhances thermal storage in mortar
- Composite PCM shows high thermal stability and 32.5 J/g latent heat capacity
- 30 wt% PCM in mortar reduces thermal conductivity by 49%
- FTIR and TGA confirm chemical and thermal stability in modified mortar
- Techno-economic analysis shows encouraging payback period of 2 years for AC_{cs}/EPCM
- Strength-thermal trade-off shows potential in insulating construction use

Thermo-Mechanical Performance and Techno-Economic Assessment of Lightweight Cement Mortar Incorporating a Coconut Shell Activated Carbon/PCM Composite for Thermal Energy Storage

M. F. Junaid [a], Z. ur Rehman [b*], C. Fabiani [c, d], C. Chiatti [c, d], M. Matejdes [e], M. Slaný [a, e*]

[a] Department of Materials Engineering and Physics, Faculty of Civil Engineering, Slovak University of Technology, Bratislava, 810 05, Slovakia

[b] School of Engineering, College of Science and Engineering, University of Derby, Derby DE22 3AW, United Kingdom

[c] EAPLAB at CIRIAF Interuniversity Research Centre on Pollution and Environment Mauro Felli, University of Perugia, Italy

[d] Department of Engineering, University of Perugia, Italy

[e] Institute of Inorganic Chemistry, Slovak Academy of Sciences, Dúbravská cesta 9, Bratislava, 845 36, Slovakia

***Corresponding Author(s)**
1. Z. ur Rehman
z.rehman1@derby.ac.uk
2. M Slaný
michal.slany@stuba.sk

Abstract: This study presents a sustainable, leakproof, shape-stable composite phase change material for Thermal Energy Storage (TES), created by incorporating a eutectic mixture of capric- and myristic-acid-based biobased PCMs into porous activated carbon derived from waste coconut shells (AC_{cs}). The resulting AC_{cs}/EPCM composite was embedded into cement mortar in varying ratios (10-30 wt%) to manufacture thermally enhanced building material. Comprehensive testing was conducted to assess the phase transition characteristics of composite PCM along with chemical, microstructural, physical, mechanical, thermal and thermophysical characterization, and thermoregulation performance evaluation of AC_{cs}/EPCM incorporated mortar. The DSC analysis showed that AC_{cs}/EPCM possessed a melting temperature of 21.8 °C and a latent heat capacity of 32.5 J/g with high thermal cycling stability. FTIR results confirmed good chemical compatibility of AC_{cs}/EPCM within cement mortar and TGA indicated sufficient thermal stability below degradation temperatures (< 150 ºC). Replacing 30 wt% of sand with composite PCM in mortar significantly enhanced its thermal insulating properties through reduction of thermal conductivity by 33% and thermal diffusivity by 26%. On the other hand, this modification led to a 75.3% decrease in compressive strength and an increase in water absorption from 7.6% to 24.7%. Further, pore size distributions of cement mortars were evaluated through mercury intrusion porosimetry indicated a reduction from 2.46 μm to 1.86 μm in critical pore diameter and increase in total porosity by 36.8% through inclusion of 30 wt% of AC_{cs}/EPCM. Furthermore, techno-economic analysis of AC_{cs}/EPCM incorporated cement mortar reveals an encouraging payback period of 2.33 years.

Keywords: Composite biobased PCM; activated carbon; cement mortar; thermal inertia; thermophysical characteristics

1. Introduction

As electricity demand continues to grow and the impacts of climate change become more severe, countries around the world are focusing on two main strategies to promote sustainability. The first is improving the energy efficiency of systems and infrastructure to reduce overall consumption. The second is shifting toward renewable energy sources to gradually move away from fossil fuels. A combination of the two approaches helps limit environmental damage while meeting energy needs. In most cases, investing in energy efficiency is more affordable at the start than increasing energy production which often requires significant capital and ongoing operating costs. By prioritizing efficiency, countries can manage energy use more effectively while laying the groundwork for a cleaner energy future [1]. Efficiency upgrades generally require less time to develop and implement compared to broader transition from fossil fuels to renewable energy sources. This is because improving energy efficiency through better technologies, materials, or systems can often be achieved within existing structures, whereas changing the energy supply typically requires overhauling infrastructure and extensive long-term planning. In 2021, the building and construction sector was responsible for 36% of global energy consumption highlighting its critical role in both energy demand and the potential for impactful efficiency improvements [2]. For instance, the majority of household energy use goes toward heating living spaces making up 63.5% of total residential energy consumption in the European Union (EU) (Fig. 1). The next largest portion is used for heating water accounting for 14.9%. Together, these two activities (i.e., space and water heating) made up 78.4% of the total energy used by households in 2022 showing that thermal comfort remains dominant energy demand in EU's residential sector [3]. As a result, enhancing energy efficiency of buildings has emerged as a key priority worldwide aiming to support sustainability goals and strengthen energy security across local, national and global scales.

The global energy crisis has also raised the demand for innovative materials capable of significantly reducing energy consumption. The integration of PCMs into building materials can improve indoor thermal comfort while reducing HVAC energy demand [4,5]. This benefit arises from the LHS capacity of PCMs, which absorb surplus heat when indoor temperature rise and release it as temperatures fall. By moderating daily temperature fluctuations, PCMs can reduce peak heating and cooling loads, maintain more stable indoor conditions, and facilitates to achieve a more uniform thermal environment within the building [6]. There are three main categories of PCMs i.e., inorganic, organic and eutectic. Organic PCMs e.g., fatty acids are widely used in building applications because they offer suitable phase transition temperatures, non-corrosiveness, chemical stability, and limited supercooling [7]. Inorganic PCMs can provide higher thermal conductivity and volumetric LHS; however, phase separation, corrosive behaviour, supercooling and reduced stability when subjected to repeated thermal cycling may limit their application [6]. On the other hand, concerns related to inorganic PCMs are fundamentally important while considering their incorporation in cementitious materials where chemical incompatibility between PCM and cement matrix can negatively affect durability and mechanical properties [6]. Although organic PCMs such as fatty acids offer several advantages, their application is limited by PCM leakage during phase transition, low thermal conductivity and inadequate shape stability when subjected to long term thermal cycles. To address aforementioned challenges, recent research has shifted its focus to different secure incorporation methods of PCMs in construction materials and building envelopes. Different techniques are available for incorporating PCMs into construction materials and building envelopes, including shape stabilization, microencapsulation, and microencapsulation [6]. Among these, shape stabilization is considered the most suitable for direct integration into construction materials. This method effectively retains the PCM within a supporting matrix, minimizing the risk of leakage during phase transitions. In addition, it eliminates the potential failures associated with capsule rupture, thereby improving the long-term durability and reliability of PCM-enhanced construction materials [7]. Thereby, research focus has been shifted to improve long term thermal reliability and structural stability of shape stabilized PCM composites [8].

Coconuts are a vital agricultural commodity in numerous tropical regions, yet the disposal of waste coconut shells remains a significant environmental concern due to the increasing global demand for coconut derived products. Annually, approximately 50 billion coconuts are cultivated worldwide with an estimated 85% of their shells discarded as waste [9]. These discarded shells are predominantly disposed of in landfills and their decomposition as organic material contributes to the emission of greenhouse gases particularly methane exacerbating climate change [10]. Additionally, improper disposal practices are linked to soil and water contamination further amplifying environmental challenges [11]. Given these issues the sustainable management and reutilization of waste coconut shells have emerged as critical priorities particularly for tropical nations where coconut production plays a pivotal role in the economy. However, the recovery and reutilization of such waste necessitate a comprehensive assessment of the distinct characteristics of the waste streams along with the selection of most effective recovery techniques [12].

The transformation of waste coconut shells into activated carbon (AC) represents an efficient and sustainable strategy to valorize agricultural residues [13]. Coconut shells being rich in lignocellulosic components serve as excellent precursors to produce high-quality AC due to their inherent carbon-rich structure [14]. Coconut shells-based AC (AC_{cs}) offers significant potential as a carrier material for PCMs in TES applications. Its large surface area and highly porous structure allow effective impregnation of PCM which stores and releases thermal energy efficiently through solid-liquid phase transition [15]. AC_{cs} utilization for TES applications facilitates the reuse of agricultural waste while offering a cost-efficient, sustainable, and eco-friendly alternative for traditional materials. [16]. This approach improves the efficiency and cost-effectiveness of TES systems by making use of the widely available and inexpensive coconut shells which contribute to sustainability. In addition, the concepts of the circular economy which include the environmental conservation and resource efficiency are compatible with the incorporation of AC_{cs} into TES applications. A number of studies [17–19] have shown that AC_{cs} encompass high surface area and porous structure which favors its utilization in TES applications based on PCMs. In addition, the carbon-based highly porous structure enhances PCM's thermal conductivity primarily due to its high surface area and interconnected pore network [20]. These porous carbon frameworks serve as thermally conductive pathways allowing heat to flow more efficiently through the composite. The extensive internal surface provides numerous contact points between the PCM and the conductive matrix which reduces thermal resistance at the interface [21]. As a result, the heat absorbed or released during phase transition is transferred more uniformly and rapidly improving the overall thermal responsiveness of the system.

Cementitious materials integrated with TES capabilities can passively regulate the temperature inside buildings. This passive solution reduces the need for energy intensive HVAC systems leading to energy savings and improving the overall energy efficiency of buildings. The implementation of such functionality involves the integration of composite PCMs into building materials [22–25]. The incorporation of shape stabilized biobased eutectic PCM (EPCM) composite (AC_{cs}/EPCM) into the cementitious mixture imparts TES characteristics. The proportion of the composite material incorporated into the cementitious mixture is decided according to the target TES capacity and the necessary mechanical properties. The equilibrium between structural integrity and TES functionality can be achieved through precise adjustments of the incorporation amounts for particular applications. Additionally, a more uniform temperature distribution can be attained by strategically placing composites within various layers of concrete [26]. The process entails the absorption and release of ambient heat by AC_{cs}/EPCM via melting and crystallization phases thereby enabling passive thermal regulation. As a result of this recurring process, reliance on conventional heating and cooling systems is reduced by improving energy efficiency and lowering costs of energy. Furthermore, the incorporation of AC_{cs}/EPCM composite in cement mortar promotes environmental sustainability by reducing the carbon footprint of structures and improving indoor thermal comfort. The chemical composition of AC_{cs} like materials includes CaO, SiO_2, Al_2O_3 and Fe_2O_3 closely resembles that of cement [27] and the high reactive silica content reacts with water and $Ca(OH)_2$ to form C-S-H gel in cementitious material [28]. Despite increasing research on PCM-based cementitious materials, an important research gap remains in the development of composites that are simultaneously low-cost, environmentally sustainable and compatible with cement-based materials while retaining sufficient mechanical performance for large scale construction applications [29]. The development of leakproof AC_{cs}/EPCM composite and its integration with TES-enabled cement mortar is critical to achieve reliable performance making this approach a compelling solution for energy efficient and sustainable construction.

Based on the previous literature evidence [30–33], this study introduces an innovative approach to waste utilization aiming to resource conservation, mitigate environmental pollution and promote circular economy through the adoption of AC/PCM composite inclusion for enhancing the energy efficiency of cement mortar. The detailed analysis of synthesized materials presents the potential for transforming waste challenges into opportunities for sustainable innovation. Although numerous porous carriers have been investigated for shape-stabilized PCMs, existing studies mainly focus on commercial ACs, expanded graphite, silica, and synthetic porous matrices. Key concerns include PCM leakage, poor interfacial compatibility with the cement matrix, loss of thermal performance during prolonged cycling, and reductions in mechanical strength. Comparatively little attention has been devoted to agricultural-waste-derived ACs, despite their potential to combine high porosity with circular-economy benefits.

Moreover, no comprehensive study has evaluated AC_{cs} as a carrier for biobased EPCM to develop PCM composite and its subsequent incorporation into cement mortar at relatively high volumetric replacement levels while simultaneously assessing thermal storage performance, pore evolution, mechanical behavior, thermal regulation, and economic feasibility. The capric–myristic acid (CA-MA) EPCM was selected in this study due to its favorable phase transition temperature which aligns well with the thermal comfort range for passive building applications [36]. Both fatty acids can be derived from renewable sources, including coconut and palm kernel oils, as well as waste cooking oils through emerging biorefinery processes. Although high-purity commercial materials were used in this study to ensure reproducibility, current purification technologies can produce biobased fatty acids of comparable quality, supporting the sustainable large-scale application of this EPCM [7,34]. Moreover, no comprehensive study has evaluated AC_{cs} as a carrier for biobased EPCM to develop PCM composite and its subsequent incorporation into cement mortar at relatively high volumetric replacement levels while simultaneously assessing thermal storage performance, pore evolution, mechanical behavior, thermal regulation, and economic feasibility. This work addresses this gap by developing a leak-proof composite based on AC_{cs} and a biobased

EPCM. Unlike conventional mineral or synthetic carrier materials, the proposed material simultaneously valorizes agricultural waste, enables passive thermal regulation, and is directly integrated into cement mortar. Beyond demonstrating thermal storage performance, the study establishes the relationships among pore structure, mechanical behavior, thermophysical properties, thermal regulation and economic feasibility, providing a comprehensive framework for evaluating sustainable TES-enabled cementitious materials.

2. Materials and methods

2.1 Materials

Steam activated powdered activated carbon produced from waste coconut shells, i.e., AC_{cs}, at activation temperature above 900 °C was procured from a commercial supplier. Steam activation involves the use of high temperature steam to create a porous structure enhancing the carbon's surface area and adsorption properties making it suitable as an appropriate carrier material. Furthermore, AC_{cs} used in this study is a food-grade material with a black color and a particle size ranging from 350-400 μm. It has a pH of approximately 5 and a bulk density of 450 kg/m^3. The AC_{cs} has a loss on drying of ≤6%, indicating low moisture content, and a residue on ignition of ≤3%. Its acid-soluble content is ≤3%, while the filtering time is approximately 70 seconds.

The EPCM was formulated by combining fatty acids with a saturated aliphatic chain of 10-14 carbon atoms [35] i.e., CA and MA. CA ($CH_3(CH_2)_8COOH$) has a density, molar mass and melting temperature range of 0.893 g/ml, 172.3 g/mol and 27-32 °C, respectively. Likewise, MA ($CH_3(CH_2)_{12}COOH$) possesses a density, molar mass and melting temperature of 0.90 g/ml, 228.4 g/mol and 56 °C, respectively. These fatty acids are considered biobased as they are derived from natural sources including both vegetable/plants based or animal oil making them environmentally friendly option [36]. Both PCMs obtained from Merck (capric acid) and Carl Roth GmbH (myristic acid) had purities ≥ 98% ensuring the reliability and consistency of the materials for experimental purposes. Moreover, all materials used in this study were utilized directly without any additional pretreatment.

The cement used for the mortar production was CEM V/A (S-P) 42.5R complies with EN 197-1 sourced from Cementerie Aldo Barbetti S.p.A., Italy. In addition, fine alluvial sand with grain size designation 0/3 mm was procured from Calcestruzzi Cipiccia S.p.A. aggregate production plant located in Narni (TR), Italy conforming to the EN 12620 and EN 13043 standards. Fig. 2 presents the sieve analysis of sand showing the percentage of material passing through each sieve size conducted in accordance with ASTM C136. Tables 1-2 enlist the manufacturer's physical, mechanical and chemical properties of the cement used for the production of cement mortar.

2.2 Specimen preparation

2.2.1 Eutectic PCM development

In selecting suitable PCM for incorporation into cementitious mixture, the thermal comfort zone was considered to determine the appropriate temperature range for phase transitions. The ideal thermal comfort conditions for indoor environments are outlined in international standards such as ISO 7730 [37] and ASHRAE 55 [38]. These standards highlight various factors that influence thermal comfort i.e., heat gain and loss, activity level, metabolic rate, relative humidity, air speed, air temperature, clothing insulation and mean radiant temperature [39]. Due to the complexity and variability of such factors, it is challenging to pinpoint a precise comfort temperature. However, based on these guidelines, the recommended ambient temperature range for thermal comfort is in the range of 20 to 28 °C [40]. Therefore, to facilitate effective functioning of PCM in building applications, the material phase transition temperature should ideally fall within this range to support optimal thermal regulation.

Based on the above-mentioned recommended phase transition temperature range, the EPCM was prepared by combining CA and MA in a specific mass ratio to achieve desired melting temperature. The melting temperatures of CA and MA through differential scanning calorimetry (DSC) were found to be 29.8 °C and 55.7 °C, respectively. The eutectic mixture was formulated by carefully selecting the appropriate mass ratio of the individual fatty acid resulting in a phase transition temperature more suitable for building interior temperature regulation. DSC analysis of the CA-MA binary mixtures identified an optimum composition of 72.5 wt% CA and 27.5 wt% MA, exhibiting a melting temperature of 20.5 °C (Fig 3). The simultaneous thermal transition of both components, together with lack of phase separation, indicates the formation of a homogeneous eutectic mixture without detectable chemical interaction or phase segregation.

2.2.2 Leak-proof composite preparation

The composite material comprising AC_{cs} and EPCM (AC_{cs}/EPCM) was prepared using a vacuum impregnation technique. The initial EPCM addition ratio was defined based on the mass of EPCM relative to the mass of AC_{cs} (EPCM/AC_{cs} × 100 (wt%)). To determine the maximum impregnation capacity of the porous AC_{cs} structure, EPCM was added at 75, 80 and 85 wt% of AC_{cs}. The impregnation process was accomplished under vacuum conditions in an advanced ATT climatic chamber (UD150C SR) at a temperature of 80°C for a period of 3h. To facilitate the proper distribution of the PCM within AC_{cs} matrix and prevent agglomeration, the mixture was periodically mixed at specific intervals during process. This stirring procedure facilitated the even dispersion of PCM throughout the pores while allowing air to enter for efficient impregnation. In their liquid state, fatty acids exhibit a surface tension in the range of 2×10^{-4} N·m^{-1} to 3×10^{-4} N·m^{-1}

which is adequate to ensure their retention within the porous structure of carrier material [41]. Therefore, the anti-leakage performance of the resulting AC_{cs}/EPCM composite was evaluated through leakage tests. The samples, each containing a specific concentration of EPCM, were heated to 60 °C, exceeding the melting point of the EPCM, for 3 hours. For leakage assessment, a molded sample was placed on a Whatman Grade 42 filter paper and carefully inspected for any visible signs of liquid leakage beneath the sample. The samples that demonstrated the highest EPCM content without leakage after 3 hours were identified with the EPCM 75 wt% and 80 wt% of AC_{cs} composites exhibiting the best anti-leakage performance (see Fig. 4). However, a slight leakage was observed in the composite with EPCM 85 wt% of AC_{cs} leading to the identification of 80 wt% as the optimum leak-proof composite for further application.

2.2.3 Mortar production

Figure 5 presents the production process of cement mortar samples. The cement mortar was prepared using a mixing ratio of sand to cement ratio of 1 and water to cement ratio of 0.75 which served as the reference mortar for comparison. To manufacture thermally efficient cement mortars (TECMs), a portion of the sand was replaced with AC_{cs}/EPCM composite at increasing weight percentages of 10%, 20% and 30%. It is pertinent to mention that the AC_{cs}/EPCM composite was incorporated by partially replacing sand, as the primary objective was to TES functionality while maintaining the cement dosage and minimizing potential effects on cement hydration, consistent with the approach reported in the literature [23]. The AC_{cs}/EPCM composite functions as a porous, aggregate-like phase, making its incorporation within the sand fraction more appropriate than direct modification of the cementitious binder. Partial replacement of sand also allows the original cement dosage and water-to-cement ratio to be maintained while introducing the PCM-containing composite into the mortar matrix. Furthermore, this approach provides thermal functionality without increasing the overall aggregate volume of the mortar. The mortars prepared with these substitutions were labeled as TECM-10%, TECM-20% and TECM-30%, respectively. Furthermore, to maintain manageable workability while optimizing the TES potential, AC_{cs}/EPCM composite substitution ratio was capped at 30%. The quantities and proportions of the ingredients used in mortar production are outlined in Table 3.

The procedure for preparing cement mortars begins by separately mixing the cement with water and the sand with composite material. The cement and water were thoroughly blended to form a smooth paste while the sand and composite were dry mixed to ensure uniform distribution. After both mixtures were prepared, the sand-composite mixture was gradually combined with cement paste and mixed thoroughly for a sufficient duration to achieve a homogeneous mortar. Subsequently, the resulting fresh mortars were poured into oiled molds with dimensions of $40 \times 40 \times 160$ mm^3 and $50 \times 50 \times 50$ mm^3 for mechanical testing and $200 \times 200 \times 15$ mm^3 for thermoregulation performance assessment. All the samples were transferred to a climatic chamber immediately after preparation and cured at 20 ± 1 °C with a relative humidity of 90% to prevent moisture loss. After one day, the samples were recovered from molds and curing was continued for 28 days. This curing process allowed the mortars to achieve their final properties for further analyses.

2.3 Testing program

2.3.1 Chemical characterization

The DRIFT (Diffuse Reflectance Infrared Fourier Transform) analysis was conducted to evaluate the structural and chemical properties of AC_{cs}/EPCM composite and mortar samples incorporating this composite. First, AC_{cs}/EPCM composite was finely ground to a powder form. A small amount of the sample was then mixed with KBr in a 1:10 weight ratio to aid in sample dilution and enhance reflectance quality. The mixture was carefully ground to homogeneous powder to ensure uniformity. Subsequently, the sample was placed in DRIFT sample holder, and spectra were collected over a specific wavenumber range i.e., 4000–400 cm^{-1}. The same procedure was repeated for prepared mortar samples containing the composite PCM allowing for comparison of the spectra and the identification of any shifts or modifications in the functional groups.

2.3.2 Microstructural characterization

A TES Vega 3 scanning electron microscope (SEM) with both secondary electron and backscattered electron detectors was used to examine the microstructure of the samples. To improve image clarity, the samples were coated with a thin layer of gold. Imaging was performed at an accelerating voltage of 20 kV which helps generate detailed surface and structural information.

2.3.3 Pore structure

Mercury intrusion porosimetry (MIP) was used to analyze the pore structure of cement-based samples. Small cube-shaped samples (1 × 1 × 1 cm^3) were tested using a Pascal 140 and 440 device (Thermo Fisher Scientific). Before the test, the samples were dried in a vacuum oven at 45 °C until their weight no longer changed ensuring all moisture and air were removed. It is pertinent to mention that the aforementioned drying temperature is well below thermal degradation temperature of EPCM used in this study, i.e., 155 °C. Moreover, the selected AC_{cs}/EPCM composite was leakproof thus EPCM remains within porous structure of AC_{cs} at this drying temperature without impacting microstructure of composite. The porosimeter had the capability to measure pore size as small as 0.003 μm and apply a maximum pressure of 414 MPa. During testing, mercury was gradually forced into the pores under increasing pressure which helped reveal even the smallest pores. For the computations, standard values for the contact angle (117°) and surface tension (0.485 $N \cdot m^{-1}$) of mercury were used from the literature as per [42,43] which are typically found for samples subjected to oven-drying. The evaluation of pore diameters was made through Washburn equation which makes the assumption that the shape of material's pores is cylindrical.

2.3.3 Physical characterization

The workability of cement mortar with and without AC_{cs}/EPCM was evaluated according to the ASTM C1437 standard. Since the control mortar was highly flowable, the mold was filled without tamping, and the remaining mortars were filled as per the aforementioned standard. After filling, the mold was carefully lifted, and the spread diameter of the mortar was measured immediately in four different directions to ensure accuracy.

The procedure for determining the water absorption and bulk density of the prepared mortar samples including those with composite PCM was conducted according to ASTM standards. In this process, mortar cubes 50 × 50 × 50 mm^3 were prepared and cured for 28 days. For water absorption (as per ASTM C642), the dry weight was first recorded. The samples were then immersed in water for 24h after which they were weighed again. The water absorption was calculated as a percentage increase in weight. For bulk density (ASTM C138), the mass of the dry samples was divided by its known volume to determine its density. A reference sample without the composite PCM was tested using the same procedure for comparison allowing for an assessment of the effect of the composite PCM on these physical properties.

2.3.4 Mechanical characterization

The compressive and flexural strength of the prepared mortar samples were evaluated following standard ASTM procedures. For compressive strength mortar cubes 50 × 50 × 50 mm^3 were prepared and tested after 28 days as per ASTM C109. Likewise, mortar prism specimens of the dimension 40 × 40 × 160 mm^3 were tested after 28 days using a three- point bending setup as specified in ASTM C348. These tests were performed on samples with and without composite PCM to determine its impact on the mechanical properties of mortar.

2.3.5 Thermal characterization

The thermal energy storage properties of the biobased EPCM and AC_{cs}/EPCM were evaluated using Differential Scanning Calorimetry (DSC) with a NETZSCH DSC 214 Polyma. The analyses were performed under a N_2 atmosphere with a flow rate of 30 ml per minute. The thermal degradation performance of the mortar samples was analyzed through thermogravimetric analysis (TGA) using a NETZSCH STA 2500 Regulus analyzer. The tests were conducted at a controlled heating rate of 5 °C per minute, with the temperature increased from ambient conditions to 500 °C while continuously monitoring the mass loss of the samples.

The thermal conductivity of the mortar samples was measured using a Hot Disk TPS 2500S instrument from Hot Disk AB, which operates according to the Transient Plan Source (TPS) method (see Fig. 6). This technique, standardized by UNI EN ISO 22007-2:2015 [44], is widely recognized for evaluating thermal properties of heterogeneous materials. During the test, a Kapton-insulated sensor (model no. 5501; radius 6.4 mm) was sandwiched between two identical mortar samples. Measurements were conducted with an output power of 50 mW and a testing time of 80s, respectively. The sensor generated a transient heat pulse while monitoring the resulting temperature response of the material, allowing for the accurate determination of the samples' thermal conductivity and related thermophysical properties. To minimize the influence of external thermal disturbances, all measurements were performed inside a dedicated polystyrene insulation box. Prior to testing, the samples were conditioned at 25 °C and 50% relative humidity for 3 hours. For this purpose, the samples were first placed inside the polystyrene box, which was subsequently stored in a climatic chamber to ensure stable environmental conditions throughout the conditioning period. After conditioning, the samples were removed from the climatic chamber and subjected to thermal conductivity measurements. To ensure consistency and accuracy, each sample was measured five times; the average value was considered to provide a reliable representation of the mortar's thermal performance.

3. Results and discussion

3.1 Chemical characterization

3.1.1 DRIFT analysis

DRIFT analysis provides important information about the structural integrity and chemical interactions of the cement mortar composite incorporating AC_{cs}/EPCM as a partial replacement for sand at 10%, 20%, and 30% levels (see Fig. 7). Several functional groups linked to carbonaceous phases, cement hydration products and PCM-derived organic compounds are represented by distinctive absorption bands in the spectra. The characteristic absorption bands confirm the successful incorporation of the AC_{cs}/EPCM composite into the cementitious matrix while preserving the typical spectral features associated with hydrated cement after 28 days of curing. No additional absorption bands indicative of new chemical reaction products were observed, suggesting that no apparent chemical incompatibility developed between the composite PCM and the cement matrix under the investigated conditions.

The broad absorption band observed between 3400 and 3600 cm^{-1} is linked to the O–H stretching vibration of water molecules. This band originates from both bound water in calcium silicate hydrate (C-S-H) gel and free water present in portlandite ($Ca(OH)_2$). The presence of this band in all specimens indicates the existence of typical hydration products after 28 days of curing. Furthermore, the H–O–H bending vibration around 1640 cm^{-1} further confirms the presence of hydration water showing that the mortar retains its typical characteristics related to moisture retention.

A key finding is the appearance of strong absorption bands between 2950 and 2850 cm^{-1} which are associated with νs and νas C–H stretching vibrations from aliphatic $–CH_2$ and $–CH_3$ groups. These bands are absent in the control sample but clearly visible in the TECM-10%, TECM-20% and TECM-30% spectra. This confirms the successful integration of AC_{cs}/EPCM composite which contains long-chain fatty acids, and the intensity of these bands increases as the composite PCM replacement level increases in cement mortar samples.

A clear indicator of composite PCM integration is the sharp absorption band around 1730 cm^{-1} which represents the C=O stretching vibration of carboxyl group (–COOH) or ester functional groups from the capric-myristic EPCM. This band did not appear in the control sample confirming that the EPCM retains its chemical distinction within the composite matrix. The presence of these ester or –COOH groups suggests that the interaction between PCM and cement was of purely physical nature rather than chemical. Therefore, PCM's ability to store and release thermal energy remained intact which enables effective thermal energy regulation in building materials.

An important observation was made through the presence of absorption bands in the 1385–1365 cm^{-1} range which are linked to carbonate (CO_3^{2-}) groups. These peaks indicate that carbonation has occurred in the mortar samples which is a common process in cement-based materials when they are exposed to atmospheric CO_2. During carbonation, CO_2 reacts with $Ca(OH)_2$ in the cement to form $CaCO_3$. This band appears in all the samples suggesting that natural carbonation took place over time. This process can actually be beneficial for the mortar's durability because it helps to fill pores within the material reducing its porosity and making the microstructure denser and more refined which can improve resistance to environmental degradation.

The Si–O stretching vibrations observed between 1100 and 950 cm^{-1} are linked to the silicate structures in C-S-H gel which is the primary binding phase in hydrated cement. The intensity of these bands is relatively comparable across all mortar samples indicating that the formation of essential cement hydration products remains intact in all specimens regardless of presence of AC_{cs}/EPCM. Moreover, it is equally important to avoid any substantial disruption in the formation of C-S-H gel which is mainly responsible for the mechanical strength of the mortar. Additionally, the absorption bands at 870–850 cm^{-1} and 750–600 cm^{-1} can be associated with carbonate compounds ($CaCO_3$) and calcium aluminate hydrate phases such as ettringite and monosulfate which are typical hydration products in cement-based materials. It is important to note that DRIFT analysis provides a qualitative assessment of typical hydration products rather than quantitative assessment. Thus, the current results should be interpreted within the qualitative assessment regime which was the main focus of the current study. The quantitative assessment of typical hydration products could be focused in future studies.

3.1.2 DSC results

The phase change behavior of both EPCM and the leak-resistant AC_{cs}/EPCM composite was examined using DSC. To ensure reliable measurements, the samples went through controlled heating and cooling cycles at a rate of 0.5 °C per minute [45]. At the extreme temperatures of –20 °C and 60 °C, the process was paused for 5 minutes. This isothermal segment made sure the material had enough time to completely melt or crystallize in each cycle. The DSC analysis was performed over two consecutive heating/cooling cycles. However, only the second cycle was considered for data evaluation in order to eliminate possible effects associated with the thermal history of the samples and instrument stabilization [45]. The selected temperature range was wide enough to guarantee complete melting and crystallization of PCM.

The DSC results of tested materials are presented in Fig. 8, while the corresponding thermal parameters are summarized in Table 4. The DSC peaks indicate heat absorption during melting (endothermic process) and heat release during crystallization (exothermic process). From these curves, the starting temperatures of phase change were identified. For EPCM, melting begins at approximately 20.5 °C, while crystallization starts at around 19.0 °C. In the case of the AC_{cs}/EPCM composite, these temperatures were slightly higher, recorded at 21.8 °C for melting and 19.1 °C for crystallization (Fig. 8). This slight increase in phase change temperature can be explained by the structure and interaction within the composite. The AC_{cs} material has a porous structure that holds the EPCM inside it. These tiny pores sometimes severely restrict the movement of the EPCM molecules, especially the long molecular chains [46]. As a result, more energy (or slightly higher temperature) is required for the molecules to rearrange themselves during melting and crystallization. In addition, forces such as surface tension and capillary action between the PCM and the AC_{cs} surface further increase the energy needed for the phase change. Another contributing factor is improved thermal conductivity in the composite. Better heat transfer allows the material to distribute heat more evenly, which can slightly shift the phase change temperature upward [47]. The interaction between the components of the composite also plays an important role in determining these thermal properties [48]. A key property evaluated in this study is the phase change enthalpy, which represents the amount of heat energy the material can store and release during the phase transition. For EPCM, the melting (ΔH_M) and crystallization (ΔH_C) enthalpies were found to be 157.2 J/g and 156.3 J/g, respectively. In comparison, the AC_{cs}/EPCM composite showed lower values of 32.5 J/g and 32.6 J/g. It is pertinent to mention that AC_{cs}/EPCM composite material showed insignificant DSC characteristics even after prolonged thermal cycling (Fig. 8c). Meanwhile, the double peaks observed during melting and crystallization after prolonged thermal cycling can be associated with subtle changes in the phase behavior of the fatty-acid-based EPCM. Similar variations have been reported for fatty-acid eutectic mixtures and are generally attributed to minor component degradation, impurities, molecular rearrangement, or partial phase separation during repeated thermal cycling. These changes can cause the individual components to undergo phase transitions over slightly different temperature ranges, resulting in the observed double peaks [49]. Overall, the results suggest that AC_{cs} is an effective supporting material for shape stabilized biobased PCM. This shows promising thermal characteristics of AC_{cs}/EPCM composite for further embedment in mortar.

3.1.3 TGA results

TGA was performed to evaluate the thermal stability of the materials (AC_{cs}, EPCM and AC_{cs}/EPCM composite) when exposed to increasing temperatures. The obtained thermograms, presented in Fig. 8, indicate mass variation as a function of temperature. Among the materials investigated, AC_{cs} showed a very strong thermal stability, with only a minor mass loss throughout the entire temperature range up to 500 °C. At lower temperatures, particularly below 100 °C, a very small weight loss was observed, which can be attributed to the evaporation of moisture that is naturally present in the material. When the temperature increased beyond 130 °C, a slight additional mass loss occurred, likely associated with the breakdown or release of some organic substances within AC_{cs}, including both volatile and non-volatile components. Nevertheless, the overall weight loss remained minimal, which confirms that AC_{cs} can withstand high temperatures without major degradation.

On the other hand, EPCM showed a single-stage (one-step) decomposition pattern. The major mass loss occurred within the temperature range of approximately 155-219 °C (Fig. 9), indicating that EPCM starts breaking down rapidly once it reaches such temperatures. The AC_{cs}/EPCM composite followed a similar decomposition trend to EPCM, even if with a significantly higher residual mass at high temperatures. The composite retained about 53% of its original mass at 500 °C. This happens because only the loaded EPCM portion in AC_{cs}/EPCM composite, i.e., 44.44% ((mass of EPCM/total mass of AC_{cs}/EPCM campsite) × 100), decomposes with approximately 2.56% impurities, while the AC_{cs} remains largely stable and intact. From these results, it can be concluded that the composite is thermally stable up to around 155 °C, i.e., when EPCM begins to decompose, which is substantially higher than its phase transition temperature (~ 21 °C) (Fig. 9). Therefore, the material can safely operate under normal conditions without any risk of thermal damage. Ultimately, the high thermal stability of the composite confirms that it can maintain its performance and structure even when exposed to temperature changes. This makes it reliable for practical applications where materials are expected to be stable under varying thermal conditions.

3.2 Microstructural characterization

3.2.1 SEM analysis

Figure 10 presents SEM images of AC_{cs}/EPCM incorporated mortar samples. It can be observed that the control specimen without AC_{cs}/EPCM shows that a needle-like structure is generated around fine cement particles indicating the formation of ettringite. These needle-like structures joined together to form a complex network bonding cement and sand particles. Also, macro and micro voids are observed within the cement-sand matrix indicating the formation of pores due to excessive water in mortar required to trigger the pozzolanic reaction responsible of generating C-S-H gel. Meanwhile, a similar structure was observed in AC_{cs}/EPCM incorporated mortar samples showing adequate needles forming a complex interjoining network. This shows that the incorporation of composite PCM in mortar samples does not completely disturb the formation of C-S-H owing to its exclusive physical presence within the cemented matrix rather than chemical. These results are also in line with FTIR which confirms the non-chemical interaction of composite PCM with cementitious matrix. Meanwhile, the flaky appearance of composite PCM becomes more and more apparent with an increase in its quantity from 10% to 30% in mortar causing hindrance for the conjunction of cement-sand particles through the joining of needles appearing on them due to the formation of C-S-H. This indicates although composite PCM is chemically inert to affect the hydration reaction within the mortar, it weakens the interfacial transition zone (ITZ) which may lead to a reduction in mechanical strength of cement mortar.

3.2.2 MIP

The pore structure of the control and TECM30% was analyzed using MIP to analyze the development of pores with the inclusion of AC_{cs}/EPCM in mortar. The pore size distribution curve of TECM-30% shows a more pronounced peak in the capillary pore region (around 1–3 µm), suggesting the formation of larger and more connected pores compared with the reference mortar. The increase in pore volume may be attributed to several factors associated with the incorporation of the AC_{cs}/EPCM composite. Firstly, the AC_{cs} possesses a highly porous structure, which can introduce additional internal voids into the mortar matrix. Secondly, replacing sand with the composite PCM reduces the packing density because the composite particles are lighter and more porous than natural sand. In addition, the reduced workability observed in PCM-incorporated mortar can lead to lower compaction and more entrapped air voids during casting. The increase in porosity may also be associated with weaker interfacial bonding between the cement paste and PCM composite particles, resulting in the formation of ITZ voids. Consequently, the TECM-30% mortar developed a less compact microstructure with higher cumulative pore volume than the control mortar. Meanwhile, the inclusion of AC_{cs}/EPCM composite increase the cumulative pore volume and leading to development of micropores thereby, increasing porosity from 22.8% to 31.2% for control and TECM-30%, respectively (Figs. 11 and 12). Furthermore, in the macroporosity region (> 0.1 µm), the final cumulative pore volume for TECM-30% remains higher than the control sample which confirms the presence of more interconnected macropores possibly due to interfacial voids and pore coalescence from the incorporation of composite PCM.

3.3 Physical characterization

The slump flow for the control sample was measured at 180 ± 5 mm. The results showed a clear trend of increased water demand as the AC_{cs}/EPCM content increased, indicating reduced workability. Composite PCM caused an increase of ~ 5.8% of water demand for the highest replacement level (i.e., 30%) to achieve sufficient workability and ease of placement as compared to 10% and 20% replacement levels while keeping constant w/c (0.75). The reason may be attributed to the high specific surface area (1350.61 m^2/g as indicated by BET analysis) [8] and porous structure of the AC_{cs} which significantly increases water absorption reducing the free water available for lubrication within the mix. Moreover, incorporating the composite PCM led to a decrease in workability. This is mainly due to its high porosity which causes it to absorb more water from the mix. Therefore, to achieve the desired flow, additional water is needed to compensate for this absorption. A similar trend was observed by [50] in which sand was partially replaced at levels up to 30%. It was observed that at 30% replacement, the water requirement increased by ~ 36% to maintain the same workability. Hashemi et al. [51] replaced the sand with highly porous material like bottom ash at levels up to 100% and observed a significant reduction in flowability reaching up to 120%. This trend was also noted by other researchers [52–54] who reported similar declines in workability when using highly porous bottom ash. However, Kim et al. [55] found that the addition of superplasticizers effectively counteracted the loss of workability in mortars containing highly porous material like bottom ash without the need to increase the water content. With the use of superplasticizers, they achieved slump flow values ranging from 150 mm to 200 mm.

3.3.1 Bulk density

Figure 13 presents the data associated with bulk density for control and TES-enabled cement mortar samples. The bulk density decreases from 1129 kg/m^3 (the control specimen) to 875 kg/m^3 (the specimen with 30% of AC_{cs}/EPCM composite). Thus, the addition of AC_{cs}/EPCM composite results in the reduction of bulk density with the largest drop of ~ 23% observed in the TECM-30% specimen. This drop in bulk density as indicated by [56] can be mainly attributed to low specific gravity (0.45 g/cm^3) and the highly porous nature of the AC_{cs} in comparison with cement (2.8 g/cm^3) and sand (2.54 g/cm^3). It is also due to the AC_{cs} having more air-filled spaces within its structure making it less dense than sand which is more compact and solid. These results are also complemented with MIP analysis which indicated increase in porosity with the incorporation of AC_{cs}/EPCM composite in mortar. A lower bulk density is crucial for reducing the overall weight of the structure which plays a significant role in the structural behavior during seismic events such as earthquakes. Mortars with bulk densities < 2000 kg/m^3 as specified by ACI PRC-213-14(23) are considered lightweight. Additionally, the bulk density of the material directly influences its thermal conductivity with lower densities typically resulting in reduced heat transfer. Moreover, a density range between 800 kg/m^3 and 1120 kg/m^3 is ideal for non-structural applications as per ACI PRC-213-14(23) which is consistent with findings by AlAbsi et al. [57] who reported a dry density of ~ 900 kg/m^3 for PCM based cement mortar. These results also suggest that the incorporation of AC_{cs}/EPCM composite can offer a viable solution for lightweight materials in construction providing both TES benefits and reduced weight for specific applications. This characteristic is beneficial not only for minimizing structural loads but also for improving the material's thermal performance, making it more suitable for energy-efficient construction.

3.3.2 Water absorption

The water absorption results indicate the potential effects of AC_{cs}/EPCM composite inclusion on the absorption capacity of mortar (see Fig. 14). In addition, water absorption also signifies its importance to determine the mechanical properties and the suitability for various applications. The control sample with a water absorption of 7.6% reflects typical behavior for untreated mortar. However, with 10% and 20% AC_{cs}/EPCM replacement the water absorption increases to 10.8% and 12.8%, respectively. This aligns with the findings by Sukontasukkul et al. [25] that demonstrate PCM's capability to improve the thermal properties in lightweight materials though often accompanied by increased water absorption with decreased mechanical strength. Furthermore, at these lower replacement levels, AC_{cs}/EPCM composite particles are likely to fit into and fill the spaces and reduce the number of accessible pores thereby decreasing water absorption. At 30% replacement level, however, water absorption rises sharply to 24.7%. This increase is due to the higher porosity associated with AC_{cs} as AC from biomass sources typically possesses substantial internal pore structures [58]. This trend confirms that while AC_{cs}/EPCM composite can enhance thermal properties, their high porosity can influence water absorption levels highlighting the importance of balancing between composite content to maintain optimal performance in water-resistant applications.

3.4 Mechanical characterization

3.4.1 Compressive strength

Compressive strength tests were conducted on both control and TECM samples after 28 days of curing. For each type of sample, three specimens were tested to failure to determine their compressive strength. The average values of compressive strengths along with their corresponding standard deviations are presented in Fig. 15 providing insights into the mechanical performance of cement mortar. The control sample exhibited a relatively high compressive strength; i.e., 26.7 MPa at 28 days. However, a noticeable reduction in compressive strength was observed in the samples containing AC_{cs}/EPCM composite. Specifically, as the proportion of composite PCM increased the compressive strength of TECMs decreased significantly as reported in the literature [59,60]. At 28-days, the compressive strengths of the TECM-10%, TECM-20% and TECM-30% samples were 21.7%, 26.6% and 75.3% lower than that of the control sample, respectively. This sharp decline in strength is attributed to the porous structure of AC_{cs} which reduces the overall density and strength of cement mortar. Additionally, the smooth surface of AC_{cs} particles leads to a weaker bond at the ITZ which is the boundary where AC_{cs} particles meet the cement paste [61]. Typically, the strength of the bond at this interface plays a crucial role in the overall mechanical properties of the cementitious material. Moreover, AC_{cs} particles do not provide sufficient surface area for a strong chemical or mechanical bond with the cement paste mainly due to relatively lack of roughness and smooth surface [62]. However, the compressive strength of novel thermally efficient cement mortar still satisfied the requirement which enables its utilization for wall plastering in non-load-bearing applications [63].

3.4.2 Flexural strength

A three-point flexural test was performed in order to assess the flexural strength of the TECM samples after 28 days of curing. Figure 16 presents the averaged flexural strength values along with the corresponding standard deviations. For the control sample, the 28-day flexural strength was measured to be 0.66 MPa. In contrast, the flexural strength of the AC_{cs}/EPCM composite incorporated TECM samples was found to be lower than that of the control sample. Moreover, an increase in composite PCM content led to a further reduction in flexural strength. Specifically, the samples with 10%, 20% and 30% composite PCM replacement demonstrated a decrease of 8.4%, 38.9% and 54.2%, respectively, in comparison with the control sample. This trend mirrors the behavior observed in compressive strength results. Previous studies have also highlighted a similar trend for instance, there was a significant reduction in both strengths with an increase in PCM content as reported by Aguiar and Félix [64]. Likewise, Vieira et al. [65] observed up to a 63.6% reduction in flexural strength for a developed composite consisting of PCM and cement relative to the reference sample. Moreover, Young et al. [66] suggested that these strengths reductions could be attributed to the thermal crack that occurs amid the hydration process affecting the material’s structural integrity.

In the current study, some key factors can be shortlisted for the reduction in mechanical characteristics of composite AC_{cs}/EPCM-based mortar as supported by previous studies [67–69]. First, the composite PCM particles themselves have inferior mechanical properties and their induction creates more voids within the mortar particularly at higher replacement levels that weakens the overall structure and subsequent reduction in mechanical strength. Second, an increase in composite PCM dosage results in higher porosity thereby increasing w/c ratio to maintain desired workability and ease of placement, e.g., in the role of insulation mortar for wall plastering. Furthermore, it is also suggested that during the mixing process, the entrapped air may also be responsible for reduced mechanical properties. Third, the existence of a weaker bond between the cementitious matrix and composite PCM particles further compromises the strength of the mortar by affecting the overall cohesion of the material.

3.5 Thermal characterization

3.5.1 TGA

TGA of the mortar samples was conducted after 28 days under a controlled heating rate of 5 °C per minute (Fig. 17). The control mortar sample exhibited three distinct phases, each corresponding to specific products formed during the hydration reactions between the cement and water. From room temperature to 100 °C, the initial minor mass loss is driven by the evaporation of free and weakly bound water within the cementitious matrix [70]. This stage involves only moisture release, with no significant chemical alterations occurring in the mortar. Between 100 °C and 200 °C, a more pronounced weight loss occurs due to the release of water chemically bound to the C-S-H gel [71]. The increasing thermal energy breaks these structural bonds, marking the initial breakdown of the material's hydration products. Finally, from 300 °C to 500 °C, the minor weight loss shown is primarily caused by the dehydroxylation of portlandite. The minimal mass reduction in this temperature range highlights the cement's high thermal resistance and excellent stability against high-temperature degradation [72].

Furthermore, TGA curves reveal a significant increase in weight loss beyond 150 °C in mortar samples containing composite PCM. This increase in mass loss shows a positive correlation with the amount of composite PCM incorporated into the mix. TECM-30% exhibited the highest weight loss as it contains the maximum replacement level of composite PCM. The observed relationship is due to the degradation of the EPCM held within the porous structure of AC. Additionally, the formation of weak bonds between the composite PCM and the cement hydrate may further contribute to the higher rate of weight loss as the thermal breakdown of the PCM is facilitated by these less stable interactions.

Overall, these results indicate that the developed TECM performs well under typical temperature conditions with the PCM effectively contributing to the material thermal management without premature degradation. The results also suggest that the integration of PCM into the mortar does not negatively impact its overall thermal stability, making it a viable option for applications requiring efficient energy storage and temperature regulation.

3.5.2 Hot disk measurements

Thermal conductivity plays a pivotal role in determining the TES capacity of the materials as highlighted by [73]. Therefore, measurement was performed using the Hot Disk measurements were performed according to the procedure mentioned in section 2.3.5. During testing, all samples were conditioned in controlled environment at 25 °C and 50% relative humidity, corresponding to the liquid phase of the EPCM, thus indicating its molten state. However, there is a controversy at this point in the literature with some studies reporting higher thermal conductivities in the liquid state [67,74], while some authors observed greater values in the solid state [24] in PCM-based mortars. For accuracy and reliability, the experimental values were calculated as the average of five repeated measurements.

The obtained thermal conductivity values are reported in Fig. 18a. A consistent decline trend was observed with increasing substitution ratio of the AC_{cs}/EPCM composite. Specifically, the thermal conductivity values for the control sample, TECM-10%, TECM-20% and TECM-30% were respectively recorded at 0.64, 0.57, 0.46 and 0.43 W/mK. Compared with the control sample, these values represent reductions of approximately 11%, 28%, and 33% for TECM-10%, TECM-20%, and TECM-30%, respectively. This behavior is consistent with previous research, e.g., [75,76]. The possible cause for this reduction can be attributed to the inherently low thermal conductivity of fatty acids (typically ranges 0.16–0.20 W/mK) [77] in comparison with the substituted mineral component; i.e., natural sand has an average thermal conductivity between 1.80–2.50 W/mK [24,78,79]. Moreover, the volume of entrapped air during the inclusion of composite PCM leads to higher porosity which is also a prominent factor for reduced thermal conductivity [80]. Previous studies [81,82] also demonstrated that a reduction in density is associated with a corresponding decrease in thermal conductivity. Rilem [83] suggests that materials with a thermal conductivity lower than 0.75 W/mK can be considered as insulating materials. According to Baite et al. [84], incorporating composite PCM in amounts greater than 30% can result in a thermal conductivity that falls below this threshold of 0.75 W/mK. This relationship is critical to assess the thermal behavior of materials particularly in applications where low thermal conductivity is desirable for enhanced energy storage or insulation properties [85]. This characteristic is advantageous for building applications where it facilitates sustained heat storage and discharge over time ensuring effective thermal regulation. In this study, the mortar with the highest composite PCM content (TECM-30%) exhibited a notable reduction in thermal conductivity (~ 50%) compared to the control mortar. This significant decrease suggests that mortars with higher composite PCM content may offer strong potential for insulation applications as reduced thermal conductivity enhances resistance to heat transfer. However, it's important to maintain a balance, while lower conductivity improves insulation, it may also slow down heat exchange, potentially limiting the effectiveness of the PCM's latent heat storage capability. Furthermore, as the proportion of AC_{cs}/EPCM composite increased, the thermal diffusivity showed a declining trend and findings are in well agreement with previous study which reported thermal diffusivity in a range of 0.2-1.2 mm^2/s (Fig. 18b) [86]. Moreover, the addition of AC_{cs}/EPCM composite to the mortar samples resulted in an increase in specific heat capacity (see Fig. 18c) and measured values were found to be within range 0.82-2.23 kJ/kgK as reported in [87]. This increasing trend in specific heat capacity can be attributed to increased amount of AC_{cs}/EPCM composite as the traditional components like cement and sand demonstrated a lower specific heat than fatty acids-based EPCM.

From the perspective of construction applications, the addition of PCM particles to the mortar layer improves its capacity to absorb and retain heat by altering its thermophysical characteristics as discussed above. The stored heat can be progressively discharged over an extended duration following the conclusion of the heating phase. Such properties provide facilitation for better alignment with fluctuating energy supply and demand offering the potential to take advantage of energy tariffs for peak and off-peak hours. This is particularly beneficial when dealing with the intermittent nature of renewable energy sources such as solar energy where energy availability may vary throughout the day. Materials that have low thermal diffusivity exhibit high thermal inertia are considered suitable substances for the purpose of insulation particularly in the construction industry. These materials are effective at resisting rapid temperature changes making them useful for maintaining stable indoor conditions. However, if the amount of PCM particles is too high, it results in substantial reduction of mortar's thermal conductivity and thermal diffusivity which is not desirable. This leads to slower heat transfer which means the heating process will take longer thereby potential increment of overall construction costs. Therefore, it is essential to determine the optimal amount of PCM to avoid imbalance between thermal performance and related construction cost.

4. Techno-economic assessment of AC_{cs}/EPCM incorporated cement mortar

A preliminary techno-economic analysis was conducted to evaluate the feasibility of employing the developed AC_{cs}/EPCM composite as a TES additive in cementitious mortars. Raw material for AC_{cs} i.e., coconut shell waste is an agricultural waste byproduct and abundantly available in many regions at low cost. Meanwhile, principal expenses related to AC production arise from thermal treatment and activation processes. Based on reported laboratory-scale manufacturing routes for biomass-derived ACs, an energy demand of approximately 3.02 kWh/kg was assumed following [88]. Vacuum impregnation was conducted using an ATT climatic chamber (UD150C SR) with a rated power of 18 kW [89] for a duration of 3 hours. In practice, the actual energy consumption is generally lower than rated power and typically ranges between 30−60%. Therefore, for the present analysis, the actual power consumption was conservatively assumed to be 50% of the rated power, corresponding to an effective power demand of 9 kW. The total energy consumption during impregnation cycle can be calculated as 27 kWh. Using a representative global residential electricity price of 0.176 $/kWh for the second quarter (Q2) of 2026 [90], the corresponding energy expenditure for producing 1 kg of AC is estimated by following equation.

$$C_{electricity} = \left(\frac{E_{total}}{m_{AC}}\right) \times P_{electricity} \quad (1)$$

where $C_{electricity}$ is electricity cost of AC production, expressed as \$/kg, E_{total} total electricity consumed during AC production, including carbonization, steam activation, washing, and drying, expressed in kWh, m_{AC} mass of activated carbon produced, expressed in kg, $\frac{E_{total}}{m_{AC}}$ is specific electricity demand for AC production expressed as kWh/kg, and $P_{electricity}$ is representative unit electricity price, expressed as $ kW/h. Considering that each impregnation batch produced approximately 3 kg of AC_{cs}/EPCM composite, the $\frac{E_{total}}{m_{AC}}$ and $C_{electricity}$ associated with the impregnation process becomes 9 kWh/kg and 1.58 $/kg, respectively. Biobased PCMs used in this study are commercially available and typically exhibit market prices ranging from 4 to 10 $/kg [91]. For the present analysis, an average cost of 7 $/kg was adopted. The total production cost of the AC_{cs}/EPCM composite can then be estimated from:

$$C_{comp} = \omega_{PCM}\, C_{PCM} + \omega_{AC} C_{AC} + C_{electricity} + C_{misc} \qquad (2)$$

where C_{comp} is the total production cost of the AC_{cs}/EPCM composite, ω_{PCM} and ω_{AC} are the mass fractions of EPCM and AC_{cs}, respectively, C_{PCM} is the PCM cost, C_{AC} is the AC production cost, $C_{electricity}$ is the impregnation cost, and C_{misc} represents miscellaneous processing costs (0.30−0.50 $/kg). Biobased PCMs used in this study are commercially available and typically exhibit C_{PCM} ranging from 4 to 10 $/kg [91]. For the present analysis, an average C_{PCM} of 7 $/kg was adopted. Thereby, for AC_{cs}/EPCM, C_{comp} was calculated to be 4.01 $/kg for loading rate of 45% as verified by TGA. It should be noted that this estimate corresponds to laboratory-scale production, where the energy consumption per unit mass is inherently higher because of the limited batch size. In industrial-scale manufacturing, larger processing capacities and improved process efficiencies would substantially reduce the specific energy consumption associated with vacuum impregnation, thereby decreasing the overall production cost. Nevertheless, even at laboratory scale, the developed AC_{cs}/EPCM composite remains competitive with several commercially available PCM-based TES materials, while simultaneously offering additional environmental benefits through the valorization of coconut shell waste and the reduction of reliance on virgin porous support materials.

Considering bulk density of TECM-30% i.e., 875 kg/m^3, the AC_{cs}/PCM composite quantity depends on the thickness of the mortar layer (t).

$$\text{Mass of } AC_{cs}/\text{EPCM } \left(\frac{\text{kg}}{\text{m}^2}\right) = 875 \times t \times 0.30 \quad (3)$$

Thus, for 10 mm thick application of mortar, C_{comp} of 4.01 \$/kg can be converted as 10.52 \$/m^2. Moreover, the additional investment associated with AC_{cs}/EPCM composite application in cement mortar for 10 mm thick layer is assumed as 0.21 \$/m^2 (2% of C_{comp}) for the optimum replacement level [92]. Thereby, the total investment for AC_{cs}/EPCM incorporated cement mortar application in buildings becomes 10.73 \$/m^2. This cost still remains competitive compared with conventional PCM technologies, such as microencapsulated PCMs and prefabricated PCM panels, which generally require more sophisticated manufacturing processes and higher application costs. Based on energy savings reported for AC based composite PCM-enhanced mortars in the literature, annual electricity savings of approximately 25−27.4 kWh/m^2 can be achievable [92]. Assuming a global average electricity tariff of 0.176 \$/kWh, the corresponding economic benefit in terms of annual savings is estimated to range between 4.4 \$/m^2 and 4.8 \$/m^2 annually. Nevertheless, detailed building-scale simulations are required to accurately quantify the operational savings associated with AC_{cs}/EPCM-incorporated mortars. The payback period can be determined from:

$$\text{Payback period} = \frac{\text{Initial investment}}{\text{Annual savings}} \quad (4)$$

The estimated payback period for proposed AC_{cs}/EPCM incorporated cement mortar is around 2.33 years. Such a short recovery period highlights the economic attractiveness of the proposed system. Following the payback period, the material is expected to continue providing economic benefits throughout its service life. Overall, the results suggest that AC_{cs}/EPCM-modified mortars constitute an economically viable TES solution for sustainable building applications.

5. Field implications

The current study evaluated the potential of incorporation of AC_{cs}/EPCM composite prepared using coconut shell waste, an abundant agricultural waste byproduct posing waste and environmental management issues, valorizing it into a high-surface-area porous carrier for biobased PCM incorporation. This approach not only provides an effective pathway for agricultural waste management but also contributes to the development of low-carbon construction materials aligned with circular economy principles. The incorporation of AC_{cs}/EPCM into cementitious mortar resulted in an enhancement of TES capabilities while maintaining acceptable mechanical performance for non-load-bearing applications. Although a gradual reduction in mechanical properties was observed with increasing AC_{cs}/EPCM dosage, the mortars retained sufficient strength for use in building envelope components, interior partition systems, renders, plasters, and other non-structural applications where thermal regulation is prioritized over high load-bearing capacity. A key contribution of this study lies in identifying an optimal AC_{cs}/EPCM incorporation level that maximizes thermal benefits while minimizing adverse effects on mechanical integrity. Such optimization is essential for the practical implementation of TES materials in cement-based systems, where an appropriate balance between structural functionality and energy performance must be achieved [93]. The thermal and mechanical performance of AC_{cs}/EPCM-incorporated mortars was found to be comparable with that of other composite PCM-based cementitious materials reported in the literature (Table 5). The results demonstrate that the developed AC_{cs}/EPCM composite provides an effective balance between thermal energy storage capability and mechanical performance, exhibiting characteristics comparable to those of existing

PCM-enhanced mortars. Compared with conventional PCM-enhanced construction materials that often rely on virgin porous supports or synthetic encapsulation systems, the proposed AC_{cs}/EPCM composite significantly improves material sustainability by employing a renewable and waste-derived precursor. This strategy reduces the environmental burden associated with raw material extraction, lowers embodied carbon, and promotes resource efficiency within the construction sector. Simultaneously, it addresses challenges associated with agricultural waste disposal, thereby creating a synergistic solution that benefits both sustainable construction practices and biomass waste valorization. From a broader perspective, AC_{cs}/EPCM-incorporated cementitious materials represent a suitable candidate for TES applications in buildings, particularly in the context of nearly zero-energy buildings, passive thermal regulation systems, and climate-responsive construction. A limitation of this study is that the effective heat storage and release capacity of the hardened AC_{cs}/EPCM mortar was not directly quantified. Although DSC confirmed the latent heat capacity of the AC_{cs}/EPCM composite, and thermal conductivity and diffusivity measurements indicated improved thermal buffering, these tests do not directly quantify the mortar's reversible TES capacity under cyclic conditions. Future work should therefore include dynamic thermal cycling and heat-flux measurements at mortar and prototype scales, together with quantitative characterization of hydration products, TGA/DTG analysis, to further establish the mechanisms governing the thermal and mechanical performance of the composite mortar and individual decomposition stages of the mortar constituents.

6. Conclusions

This study proposes a novel recycling method for coconut shell waste in shape stabilized composite biobased PCM for TES infused lightweight mortar, to promote clean energy in building sector and waste valorization and contributing to key sustainable development goals. To this end, a AC_{cs}/EPCM composite was produced and incorporated in lightweight mortar. To further evaluate this AC_{cs}/EPCM based lightweight composite, microstructural, physical, mechanical, thermophysical and thermoregulation performance were investigated through incorporating varying amounts of shape stable composite PCM. The adopted composite PCM was entirely biobased making it an environmentally friendly option for developing TES systems with a smaller ecological footprint.

In the initial phase of this study, mortar samples were produced with varying content of shape stable composite PCM at fixed water to cement ratio of 0.75. The introduction of composite PCM led to a notable increase in water demand (~ 5.8%) and decrease in workability compared with control mortar.

Microstructural analysis was conducted on mortar samples with and without composite PCM. SEM analysis revealed that the composite PCM particles were uniformly and finely distributed throughout the material. The incorporation of composite PCM led to a decrease in the density and an increase in the water-accessible porosity of the mortars. This can be attributed to both the additional water required for workability control and the air trapped during the mixing process. Furthermore, thermogravimetric analysis indicated changes in the composition of cement hydrate for the composite PCM based mortars.

The incorporation of composite PCM altered the pore structure of the cement mortars. The inclusion of composite PCM caused a significant decrease in critical pore size. Subsequently, there was an increase in total porosity than control mortar as indicated by MIP. The results also indicated that incorporating composite PCM into the mortar led to an increase in porosity encompassing micro, meso and macropores.

The mechanical properties of the cement mortars were significantly influenced by the incorporation of composite PCM. A reduction of approximately 21.7% in the compressive strength was observed with the addition of 10 wt% composite PCM. However, the PCM based mortars maintained the required strength necessary for non-structural applications as long as the composite PCM content remained up to 30 wt%.

On the other hand, the inclusion of the composite PCM significantly enhanced the thermal resistance of the cement mortars. For instance, a reduction of approximately 33% in thermal conductivity was observed in TECM-30%. This improvement is likely due to both the inherent thermal properties of the composite PCM and the increased porosity of the TECMs compared to the control mortar.

Techno-economic analysis of AC_{cs}/EPCM incorporated cement mortar shows a payback period of 2.33 years with total cradle to gate plastering application cost of 10.72 \$/m^2 making it a cost-effective TES solution for building applications with additional benefits of coconut shell waste valorization.

The current study concludes that the TECM-30% composition demonstrated a promising balance between mechanical and thermal properties. In contrast, mortars with higher composite PCM content should be regarded as materials intended for coating or filling applications rather than for structural purposes owing to its reduced mechanical characteristics.

Acknowledgement:

This work was supported by the Slovak Research and Development Agency under the Contract No. APVV-24-0133 and Slovak Grant Agency VEGA (Grant No. 1/0278/25).

References

[1] A.I. Osman, L. Chen, M. Yang, G. Msigwa, M. Farghali, S. Fawzy, D.W. Rooney, P.-S. Yap, Cost, environmental impact, and resilience of renewable energy under a changing climate: a review, Environ. Chem. Lett. 21 (2023) 741–764.

[2] United Nations Environment Programme, 2021 Global Status Report for Buildings and Construction, 2021, Available at 〈https://globalabc.org/sites/default/files/2021-10/GABC_Buildings-GSR-2021_BOOK.pdf〉, 2021.

[3] T.S. TSEMEKIDI, P. BERTOLDI, D. DAGOSTINO, L. CASTELLAZZI, C. MADUTA, E. CLEMENTI, D. PACI, V.N. DELLA, I. SAVIUC, Energy Consumption and Energy Efficiency trends in the EU, 2000-2022, (2025).

[4] K. Zhong, S. Li, G. Sun, S. Li, X. Zhang, Simulation study on dynamic heat transfer performance of PCM-filled glass window with different thermophysical parameters of phase change material, Energy Build. 106 (2015) 87–95. https://doi.org/10.1016/J.ENBUILD.2015.05.014.

[5] J. Lizana, R. Chacartegui, A. Barrios-Padura, C. Ortiz, Advanced low-carbon energy measures based on thermal energy storage in buildings: A review, Renewable and Sustainable Energy Reviews 82 (2018) 3705–3749. https://doi.org/10.1016/J.RSER.2017.10.093.

[6] M.F. Junaid, Z. ur Rehman, M. Čekon, J. Čurpek, R. Farooq, H. Cui, I. Khan, Inorganic phase change materials in thermal energy storage: A review on perspectives and technological advances in building applications, Energy Build. 252 (2021) 111443. https://doi.org/10.1016/J.ENBUILD.2021.111443.

[7] M.F. Junaid, Z. ur Rehman, N. Ijaz, R. Farooq, U. Khalid, Z. Ijaz, Performance evaluation of cement-based composites containing phase change materials from energy management and construction standpoints. Construction and Building Materials 416 (2024): 135108.

[8] M.F. Junaid, Z. ur Rehman, C. Fabiani, M. Slaný, Coconut shell waste based activated carbon as a scaffolding of biobased phase change material for enhanced thermal energy storage: Sustainable waste recycling for renewable energy source, Journal of Building Engineering 125 (2026) 116129. https://doi.org/10.1016/J.JOBE.2026.116129.

[9] M. Wahab, I.N.R. Zaim, H.F. Ismail, N. Othman, H. Hara, F.N.M. Akhir, Evaluation of flavonoid compound in coconut waste and its antioxidant activity, in: IOP Conf. Ser. Earth Environ. Sci., IOP Publishing, 2023: p. 12006.

[10] J.D. Maasakkers, D.J. Varon, A. Elfarsdóttir, J. McKeever, D. Jervis, G. Mahapatra, S. Pandey, A. Lorente, T. Borsdorff, L.R. Foorthuis, Using satellites to uncover large methane emissions from landfills Sci, Adv 8 (2022) 10–1126.

[11] O.I. Ogidi, S.C. Izah, Water Contamination by Municipal Solid Wastes and Sustainable Management Strategies, in: Water Crises and Sustainable Management in the Global South, Springer, 2024: pp. 313–339.

[12] M. Harja, C. Teodosiu, D.N. Isopescu, O. Gencel, D. Lutic, G. Ciobanu, I. Cretescu, Using fly ash wastes for the development of new building materials with improved compressive strength, Materials 15 (2022) 644.

[13] P. Tittelein, S. Gibout, E. Franquet, L. Zalewski, D. Defer, Identification of thermal properties and thermodynamic model for a cement mortar containing PCM by using inverse method, Energy Procedia 78 (2015) 1696–1701.

[14] S.W. Sharshir, A. Joseph, M. Elsharkawy, M.A. Hamada, A.W. Kandeal, M.R. Elkadeem, A.K. Thakur, Y. Ma, M.E. Moustapha, M. Rashad, Thermal energy storage using phase change materials in building applications: A review of the recent development, Energy Build. 285 (2023) 112908.

[15] M.A. Jafari, N. Attan, M.S. Tabish, A. Amarkhil, Preparation and thermal behavior of palmitic acid/activated carbon from corncob as phase change materials for thermal energy storage, J. Therm. Anal. Calorim. 148 (2023) 9453–9464.

[16] G. Predeanu, V. Slăvescu, M.F. Drăgoescu, N.M. Bălănescu, A. Fiti, A. Meghea, P. Samoila, V. Harabagiu, M. Ignat, A.-M. Manea-Saghin, Green synthesis of advanced carbon materials used as precursors for adsorbents applied in wastewater treatment, Materials 16 (2023) 1036.

[17] I.P. Vali, B.S. Anusha, M. Pruthvija, S. Savitha, S. Ravindra, M. Nagaveni, P.S. Poojitha, N. Swathi, Bamboo and coconut shell based activated carbon: A Raman spectroscopic study, Mater. Chem. Phys. 318 (2024) 129240.

[18] M. Tomy, G.S. Geethamma, A.M. Aravind, S.S. Reshmi, X.T. Suryabai, Effect of activation environment on coconut-husk-derived porous activated carbon for renewable energy storage applications, ACS Sustainable Resource Management 1 (2024) 1534–1547.

[19] M.K. Singla, J. Gupta, M. Safaraliev, P. Nijhawan, A.S. Oberoi, A.A. Menaem, Characterization of an activated carbon electrode made from coconut shell precursor for hydrogen storage applications, Int. J. Hydrogen Energy 61 (2024) 1417–1428.

[20] D.G. Atinafu, W. Dong, X. Huang, H. Gao, G. Wang, Introduction of organic-organic eutectic PCM in mesoporous N-doped carbons for enhanced thermal conductivity and energy storage capacity, Appl. Energy 211 (2018) 1203–1215.

[21] M. Wang, P. Li, F. Yu, Hierarchical porous carbon foam-based phase change composite with enhanced loading capacity and thermal conductivity for efficient thermal energy storage, Renew. Energy 172 (2021) 599–605.

[22] L.F. Cabeza, C. Castellon, M. Nogues, M. Medrano, R. Leppers, O. Zubillaga, Use of microencapsulated PCM in concrete walls for energy savings, Energy Build. 39 (2007) 113–119.

[23] H. Yang, Z. Xu, H. Cui, X. Bao, W. Tang, G. Sang, X. Chen, Cementitious composites integrated phase change materials for passive buildings: An overview, Constr. Build. Mater. 361 (2022) 129635.

[24] V.D. Cao, S. Pilehvar, C. Salas-Bringas, A.M. Szczotok, J.F. Rodriguez, M. Carmona, N. Al-Manasir, A.-L. Kjøniksen, Microencapsulated phase change materials for enhancing the thermal performance of Portland cement concrete and geopolymer concrete for passive building applications, Energy Convers. Manag. 133 (2017) 56–66.

[25] P. Sukontasukkul, P. Uthaichotirat, T. Sangpet, K. Sisomphon, M. Newlands, A. Siripanichgorn, P. Chindaprasirt, Thermal properties of lightweight concrete incorporating high contents of phase change materials, Constr. Build. Mater. 207 (2019) 431–439.

[26] W. Ke, J. Ji, C. Zhang, H. Xie, Y. Tang, C. Wang, Effects of the PCM layer position on the comprehensive performance of a built-middle PV-Trombe wall system for building application in the heating season, Energy 267 (2023) 126562.

[27] Vijay Kumar; Prince Sharma, An experimental research on the strength characteristics of concrete with ground nut shell ash, fly ash and coconut shell ashas partial replacement of cement, International Journal of Innovative Technology and Exploring Engineering (IJITEE) 8 (2019) 2278–3075.

[28] V. Charitha, V.S. Athira, V. Jittin, A. Bahurudeen, P. Nanthagopalan, Use of different agro-waste ashes in concrete for effective upcycling of locally available resources, Constr. Build. Mater. 285 (2021) 122851.

[29] A. Vedrtnam, K. Kalauni, N. Soares, B. Salazar, C.P. Ostertag, H.K. Taylor, Phase change materials for climate-adaptive buildings: A review framed by tropical and Mediterranean climates, J. Energy Storage 125 (2025) 116938. https://doi.org/10.1016/J.EST.2025.116938.

[30] M. Mehrali, S.T. Latibari, M. Mehrali, H.S.C. Metselaar, M. Silakhori, Shape-stabilized phase change materials with high thermal conductivity based on paraffin/graphene oxide composite, Energy Convers. Manag. 67 (2013) 275–282. https://doi.org/10.1016/J.ENCONMAN.2012.11.023.

[31] S. Ramakrishnan, X. Wang, J. Sanjayan, J. Wilson, Assessing the feasibility of integrating form-stable phase change material composites with cementitious composites and prevention of PCM leakage, Mater. Lett. 192 (2017) 88–91. https://doi.org/10.1016/J.MATLET.2016.12.052.

[32] P. Uthaichotirat, P. Sukontasukkul, P. Jitsangiam, C. Suksiripattanapong, V. Sata, P. Chindaprasirt, Thermal and sound properties of concrete mixed with high porous aggregates from manufacturing waste impregnated with phase change material, Journal of Building Engineering 29 (2020). https://doi.org/10.1016/j.jobe.2019.101111.

[33] Y.U. Kim, S. Yang, S. Kim, Thermal characteristics of cementitious building materials with carbon and PCM for improved heat storage performance, Constr. Build. Mater. 449 (2024) 138550. https://doi.org/10.1016/J.CONBUILDMAT.2024.138550.

[34] W. Lee, J. Lee, W. Yang, J. Kim, Fabrication of Biobased Advanced Phase Change Material and Multifunctional Composites for Efficient Thermal Management, ACS Sustain. Chem. Eng. 11 (2023) 1178–1189. https://doi.org/10.1021/ACSSUSCHEMENG.2C06598.

[35] M. Bragaglia, F.R. Lamastra, J.A. Berrocal, L. Paleari, F. Nanni, Sustainable phase change materials (PCMs): waste fat from cooking pork meat confined in polypropylene fibrous mat from waste surgical mask and porous bio-silica, Materials Today Sustainability 23 (2023) 100454.

[36] M.F. Junaid, Z. ur Rehman, N. Ijaz, M. Čekon, J. Čurpek, A.B. Elhag, Biobased phase change materials from a perspective of recycling, resources conservation and green buildings, Energy Build. (2022) 112280.

[37] E.N. ISO, 7730: 2005 Ergonomics of the thermal environment, Analytical Determination and Interpretation of Thermal Comfort Using Calculation of the PMV and PPD Indices and Local Thermal Comfort Criteria (2005).

[38] A. ANSI, M. Ashrae, Standard 55—thermal environmental conditions for human occupancy, ASHRAE, Atlanta (2004).

[39] K. Cellat, B. Beyhan, C. Güngör, Y. Konuklu, O. Karahan, C. Dündar, H. Paksoy, Thermal enhancement of concrete by adding bio-based fatty acids as phase change materials, Energy Build. 106 (2015) 156–163.

[40] B.Y. Yun, Y. Kang, Y.U. Kim, S. Wi, S. Kim, Practical solutions with PCM for providing thermal stability of temporary house, school and hospital in disaster situations, Build. Environ. 207 (2022) 108540.

[41] D. Rozanna, T.G. Chuah, A. Salmiah, T.S.Y. Choong, M. Sa'Ari, Fatty acids as phase change materials (PCMs) for thermal energy storage: a review, Int. J. Green Energy 1 (2005) 495–513.

[42] D. Shi, D.N. Winslow, Contact angle and damage during mercury intrusion into cement paste, Cem. Concr. Res. 15 (1985) 645–654.

[43] A.A. Liabastre, C. Orr, An evaluation of pore structure by mercury penetration, J. Colloid Interface Sci. 64 (1978) 1–18.

[44] S. Malinarič, P. Bokes, Impact of the heat source model on transient methods of conductivity and diffusivity measurement, Int. J. Thermophys. 43 (2022) 1–16.

[45] J.V. Christy, A. Balwani, H. Mehling, N. Agrawal, Optimization of DSC measurements for organic phase change materials, J. Energy Storage 73 (2023) 109032. https://doi.org/10.1016/J.EST.2023.109032.

[46] P. Ong, S. Goh, Y. Leow, S. Wang, … P.W.-J. of C., undefined 2024, Valorization of coconut peat to develop a novel shape-stabilized phase change material for thermal energy storage, ElsevierPJ Ong, SHA Goh, Y Leow, S Wang, P Wang, Z Li, X Yin, BH Tan, W Thitsartarn, J XuJournal of Cleaner Production, 2024•Elsevier (n.d.).

https://www.sciencedirect.com/science/article/pii/S0959652624009168 (accessed May 9, 2026).

[47] A. Muchtar, C. Hassam, … B.S.-J. of E., undefined 2022, Shape-stabilized phase change materials: Performance of simple physical blending synthesis and the potential of coconut based materials, ElsevierAR Muchtar, CL Hassam, B Srinivasan, D Berthebaud, T Mori, N Soelami, B YuliartoJournal of Energy Storage, 2022•Elsevier (n.d.). https://www.sciencedirect.com/science/article/pii/S2352152X2200980X (accessed May 9, 2026).

[48] P. Gallart-Sirvent, M.M. Martín, G. Villorbina, M. Mercè Balcells, A. Soí, C. Barrenche, L.F. Cabeza, R. Canela-Garayoa, Fatty acid eutectic mixtures and derivatives from non-edible animal fat as phase change materials, Pubs.Rsc.OrgP Gallart-Sirvent, M Martín, G Villorbina, M Balcells, A Solé, C Barrenche, LF CabezaRSC Advances, 2017•pubs.Rsc.Org (2017). https://doi.org/10.1039/c7ra03845c.

[49] M. Nazari, M. Jebrane, N. Terziev, Multicomponent bio-based fatty acids system as phase change material for low temperature energy storage, J. Energy Storage 39 (2021) 102645. https://doi.org/10.1016/j.est.2021.102645.

[50] Y. Aggarwal, R. Siddique, Microstructure and properties of concrete using bottom ash and waste foundry sand as partial replacement of fine aggregates, Constr. Build. Mater. 54 (2014) 210–223.

[51] S.S.G. Hashemi, H. Bin Mahmud, J.N.Y. Djobo, C.G. Tan, B.C. Ang, N. Ranjbar, Microstructural characterization and mechanical properties of bottom ash mortar, J. Clean. Prod. 170 (2018) 797–804.

[52] S. Gooi, A.A. Mousa, D. Kong, A critical review and gap analysis on the use of coal bottom ash as a substitute constituent in concrete, J. Clean. Prod. 268 (2020) 121752.

[53] A.S. Cadersa, I. Auckburally, Use of unprocessed coal bottom ash as partial fine aggregate replacement in concrete, University of Mauritius Research Journal 20 (2014) 62–84.

[54] M. Rafieizonooz, J. Mirza, M.R. Salim, M.W. Hussin, E. Khankhaje, Investigation of coal bottom ash and fly ash in concrete as replacement for sand and cement, Constr. Build. Mater. 116 (2016) 15–24.

[55] H.-K. Kim, J.H. Jeon, H.-K. Lee, Flow, water absorption, and mechanical characteristics of normal-and high-strength mortar incorporating fine bottom ash aggregates, Constr. Build. Mater. 26 (2012) 249–256.

[56] C.O. Chin, X. Yang, S.C. Paul, L.S. Wong, S.Y. Kong, Development of thermal energy storage lightweight concrete using paraffin-oil palm kernel shell-activated carbon composite, J. Clean. Prod. 261 (2020) 121227.

[57] Z.A. Al-Absi, M.I.M. Hafizal, M. Ismail, H. Awang, A. Al-Shwaiter, Properties of PCM-based composites developed for the exterior finishes of building walls, Case Studies in Construction Materials 16 (2022) e00960.

[58] A.R. Muchtar, C.L. Hassam, B. Srinivasan, D. Berthebaud, T. Mori, N. Soelami, B. Yuliarto, Shape-stabilized phase change materials: Performance of simple physical blending synthesis and the potential of coconut based materials, J. Energy Storage 52 (2022) 104974.

[59] A. D'Alessandro, A.L. Pisello, C. Fabiani, F. Ubertini, L.F. Cabeza, F. Cotana, Multifunctional smart concretes with novel phase change materials: Mechanical and thermo-energy investigation, Appl. Energy 212 (2018) 1448–1461.

[60] H.-W. Min, S. Kim, H.S. Kim, Investigation on thermal and mechanical characteristics of concrete mixed with shape stabilized phase change material for mix design, Constr. Build. Mater. 149 (2017) 749–762.

[61] Z. Dong, H. Cui, W. Tang, D. Chen, H. Wen, Development of hollow steel ball macro-encapsulated PCM for thermal energy storage concrete, Materials 9 (2016) 59.

[62] A. Yousefi, W. Tang, M. Khavarian, C. Fang, Development of novel form-stable phase change material (PCM) composite using recycled expanded glass for thermal energy storage in cementitious composite, Renew. Energy 175 (2021) 14–28.

[63] M. Syarif, A.R. Nanda, H. Al Imran, N. Karim, A. Yusri, Compressive Strength Analysis of Renewable Mortar after Portland Cement Replacement with Waste Ash, Engineering, Technology & Applied Science Research 14 (2024) 15056–15061.

[64] M. Félix, J.L. Aguiar, Study of a cement mortar with incorporation of PCM microcapsules, (2009).

[65] J. Vieira, L. Senff, H. Gonçalves, L. Silva, V.M. Ferreira, J.A. Labrincha, Functionalization of mortars for controlling the indoor ambient of buildings, Energy Build. 70 (2014) 224–236.

[66] B.A. Young, G. Falzone, Z. She, A.M. Thiele, Z. Wei, N. Neithalath, G. Sant, L. Pilon, Early-age temperature evolutions in concrete pavements containing microencapsulated phase change materials, Constr. Build. Mater. 147 (2017) 466–477.

[67] T. Lecompte, P. Le Bideau, P. Glouannec, D. Nortershauser, S. Le Masson, Mechanical and thermo-physical behaviour of concretes and mortars containing phase change material, Energy Build. 94 (2015) 52–60.

[68] Z.I. Djamai, F. Salvatore, A.S. Larbi, G. Cai, M. El Mankibi, Multiphysics analysis of effects of encapsulated phase change materials (PCMs) in cement mortars, Cem. Concr. Res. 119 (2019) 51–63.

[69] G. Li, G. Xu, J. Zhang, Experimental investigation of thermal and mechanical characteristics of slag cement mortars with PCM for radiant floors, Case Studies in Construction Materials 20 (2024) e02958.

[70] G. Li, G. Xu, Z. Tao, Effect on the thermal properties of building mortars with microencapsulated phase change materials for radiant floors, Buildings 13 (2023) 2476.

[71] I. Asadi, M.H. Baghban, M. Hashemi, N. Izadyar, B. Sajadi, Phase change materials incorporated into geopolymer concrete for enhancing energy efficiency and sustainability of buildings: A review, Case Studies in Construction Materials 17 (2022) e01162.

[72] L. Alarcon-Ruiz, G. Platret, E. Massieu, A. Ehrlacher, The use of thermal analysis in assessing the effect of temperature on a cement paste, Cem. Concr. Res. 35 (2005) 609–613.

[73] C. Ma, Y. Zhang, X. Chen, X. Song, K. Tang, Experimental Study of an Enhanced Phase Change Material of Paraffin/Expanded Graphite/Nano-Metal Particles for a Personal Cooling System, Materials 2020, Vol. 13, Page 980 13 (2020) 980. https://doi.org/10.3390/MA13040980.

[74] F. Alassaad, K. Touati, D. Levacher, N. Sebaibi, Impact of phase change materials on lightened earth hygroscopic, thermal and mechanical properties, Journal of Building Engineering 41 (2021) 102417.

[75] A. Joulin, L. Zalewski, S. Lassue, H. Naji, Experimental investigation of thermal characteristics of a mortar with or without a micro-encapsulated phase change material, Appl. Therm. Eng. 66 (2014) 171–180.

[76] E. Franquet, S. Gibout, P. Tittelein, L. Zalewski, J.-P. Dumas, Experimental and theoretical analysis of a cement mortar containing microencapsulated PCM, Appl. Therm. Eng. 73 (2014) 32–40.

[77] M. Nazari, M. Jebrane, N. Terziev, Multicomponent bio-based fatty acids system as phase change material for low temperature energy storage, J. Energy Storage 39 (2021) 102645.

[78] H. Cui, W. Liao, X. Mi, T.Y. Lo, D. Chen, Study on functional and mechanical properties of cement mortar with graphite-modified microencapsulated phase-change materials, Energy Build. 105 (2015) 273–284.

[79] A.M. Borreguero, I. Garrido, J.L. Valverde, J.F. Rodríguez, M. Carmona, Development of smart gypsum composites by incorporating thermoregulating microcapsules, Energy Build. 76 (2014) 631–639.

[80] M. Fenollera, J.L. Míguez, I. Goicoechea, J. Lorenzo, M. Ángel Álvarez, The influence of phase change materials on the properties of self-compacting concrete, Materials 6 (2013) 3530–3546.

[81] M. Aguayo, S. Das, C. Castro, N. Kabay, G. Sant, N. Neithalath, Porous inclusions as hosts for phase change materials in cementitious composites: Characterization, thermal performance, and analytical models, Constr. Build. Mater. 134 (2017) 574–584.

[82] C.O. Chin, X. Yang, S.C. Paul, L.S. Wong, S.Y. Kong, Development of thermal energy storage lightweight concrete using paraffin-oil palm kernel shell-activated carbon composite, J. Clean. Prod. 261 (2020) 121227.

[83] L.C. Rilem, Functional classification of lightweight concrete, Mater. Struct 11 (1978) e283.

[84] E. Baite, A. Messan, K. Hannawi, F. Tsobnang, W. Prince, Physical and transfer properties of mortar containing coal bottom ash aggregates from Tefereyre (Niger), Constr. Build. Mater. 125 (2016) 919–926.

[85] U.J. Alengaram, B.A. Al Muhit, M.Z. bin Jumaat, Utilization of oil palm kernel shell as lightweight aggregate in concrete–A review, Constr. Build. Mater. 38 (2013) 161–172.

[86] G. Li, G. Xu, J. Zhang, Experimental investigation of thermal and mechanical characteristics of slag cement mortars with PCM for radiant floors, Case Studies in Construction Materials 20 (2024) e02958.

[87] C.O. Chin, Y.K. Sih, Thermal Properties of Concrete Incorporated with Shape-stable Phase Change Material, in: MATEC Web of Conferences, EDP Sciences, 2018: p. 06021.

[88] J. Saleem, Z.K.B. Moghal, F. Tahir, G. McKay, Life cycle and energy implications of tubular vs chamber furnace pyrolysis for activated carbon production, Results in Engineering 31 (2026) 111472. https://doi.org/10.1016/J.RINENG.2026.111472.

[89] Altitude acstestchambers.com, n.d.

[90] Electricity prices around the world | GlobalPetrolPrices.com, (n.d.). https://www.globalpetrolprices.com/electricity_prices/ (accessed July 4, 2026).

[91] S. Dora, F. Kuznik, M.K. Madhavan, Phase change materials for buildings’ thermal energy management: an overview, Thermal Science and Engineering Progress 71 (2026) 104521. https://doi.org/10.1016/J.TSEP.2026.104521.

[92] E. Timurkaynak, A. Sarı, A. Güllü, M. Nas, O. Gencel, A. Ustaoğlu, H. Arslanoğlu, V. V. Tyagi, Engineering shape-stabilized pomegranate peel-derived Biochar-PCM incorporating cement mortars for passive thermal regulation in sustainable buildings, Journal of Building Engineering 127 (2026) 116348. https://doi.org/10.1016/J.JOBE.2026.116348.

[93] B.M. Tripathi, S.K. Shukla, Experimental investigation of bio-based PCM for energy-efficient building envelopes, Advances in Building Energy Research (2026) 1–26. https://doi.org/10.1080/17512549.2026.2614759.

[94] S. Ramakrishnan, X. Wang, J. Sanjayan, J. Wilson, Thermal Energy Storage Enhancement of Lightweight Cement Mortars with the Application of Phase Change Materials, Procedia Eng. 180 (2017) 1170–1177. https://doi.org/10.1016/J.PROENG.2017.04.277.

[95] T. Qian, J. Li, Octadecane/C-decorated diatomite composite phase change material with enhanced thermal conductivity as aggregate for developing structural–functional integrated cement for thermal energy storage, Energy 142 (2018) 234–249. https://doi.org/10.1016/J.ENERGY.2017.10.021.

[96] D. Sun, L. Wang, Utilization of paraffin/expanded perlite materials to improve mechanical and thermal properties of cement mortar, Constr. Build. Mater. 101 (2015) 791–796. https://doi.org/10.1016/J.CONBUILDMAT.2015.10.123.

[97] Z. Zhang, G. Shi, S. Wang, X. Fang, X. Liu, Thermal energy storage cement mortar containing n-octadecane/expanded graphite composite phase change material, Renew. Energy 50 (2013) 670–675. https://doi.org/10.1016/J.RENENE.2012.08.024.

[98] S. Liao, H. Xu, H. Zhang, K. Ma, X. Jiang, Z. Zhao, Composite energy storage cement-based mortar including coal gasification slag/paraffin shape-stabilized phase change material: physical, mechanical, thermal properties, Journal of Building Engineering 95 (2024) 110327. https://doi.org/10.1016/J.JOBE.2024.110327.

[99] M. Li, Z. Wu, J. Tan, Heat storage properties of the cement mortar incorporated with composite phase change material, Appl. Energy 103 (2013) 393–399. https://doi.org/10.1016/J.APENERGY.2012.09.057.

[100] Q. Xu, K. Zhu, X. Zhang, W. Yang, J. Rao, M. Liu, Comparative study of KOH and H_3PO_4 activated Lvzhou No. 1-based shape-stabilized phase change materials: Properties and potential application in phosphogypsum, Constr. Build. Mater. 476 (2025) 141225. https://doi.org/10.1016/J.CONBUILDMAT.2025.141225.

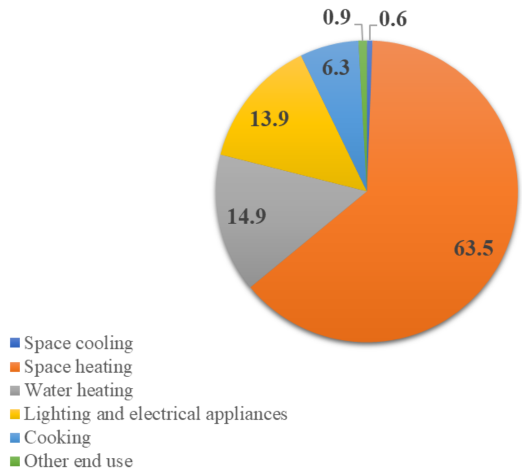

Fig. 1. Percentage share of energy consumption in EU households [3]

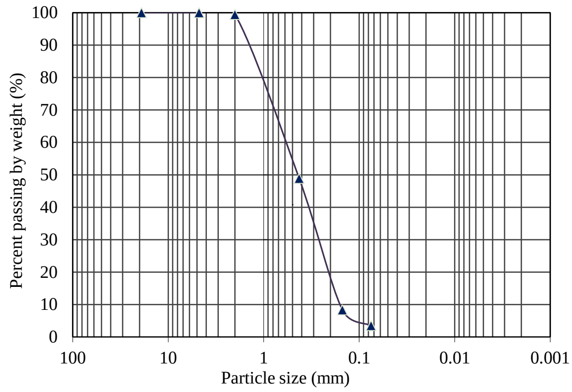

Fig. 2. Particle size distribution curve of sand

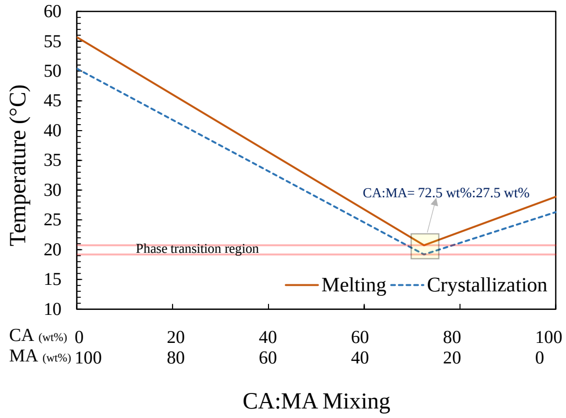

Fig 3: Preparation of EPCM using DSC outcomes of CA:MA mix ratios

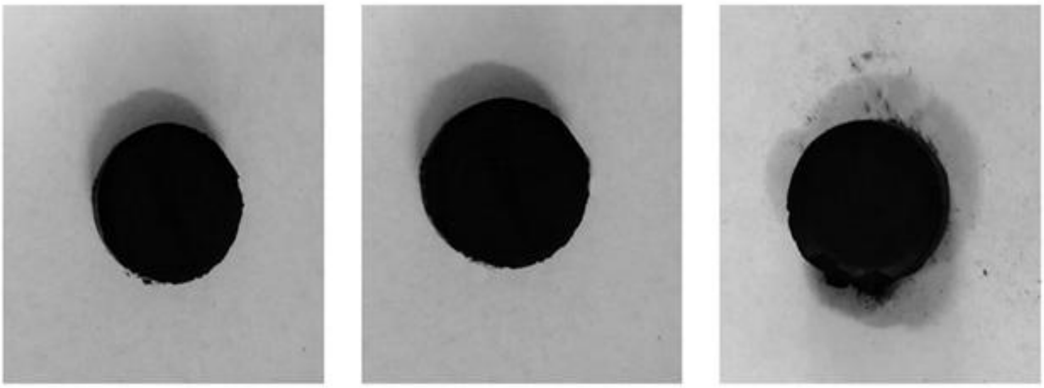

AC_{cs}/EPCM (75 wt%) **AC_{cs}/EPCM (80 wt%)** **AC_{cs}/EPCM (85 wt%)**

Fig. 4. Leakage test results of AC_{cs}/EPCM composites prepared with different initial PCM mixing (75, 80, and 85 wt% of AC_{cs}) during the vacuum impregnation process.

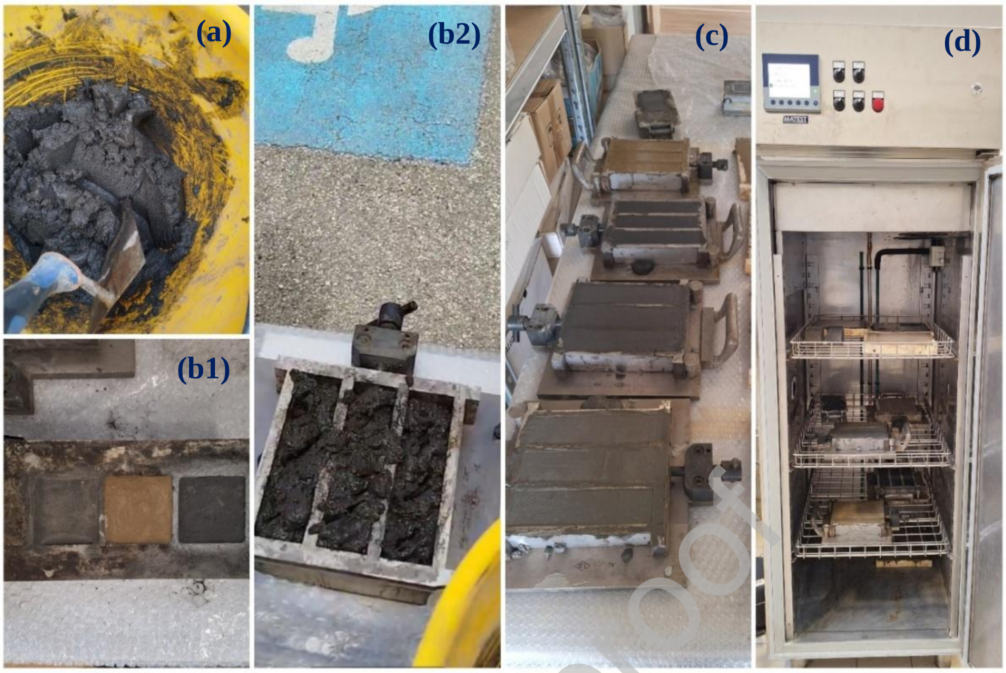

Fig. 5. Production process of the produced mortars with/without AC_{cs}/EPCM composite (a) mixing; (b1-2) molding; (c) molded samples; (d) curing in environmental chamber

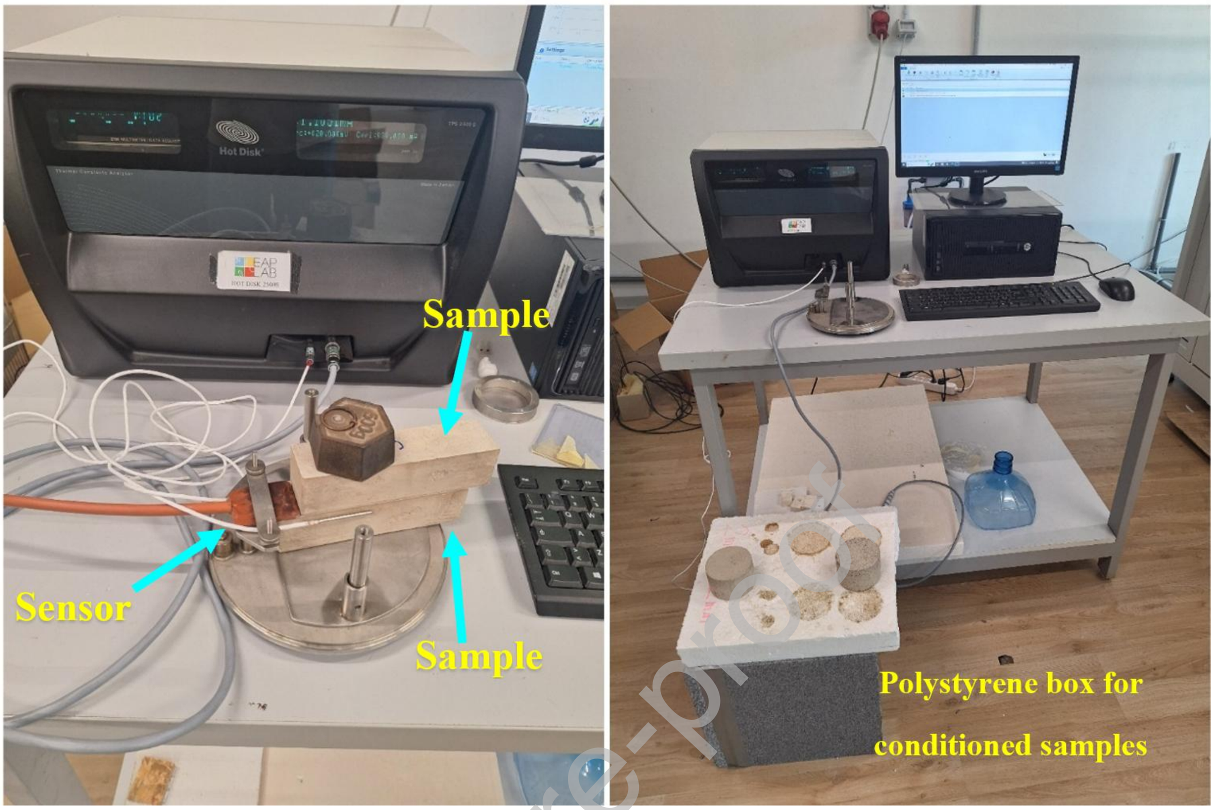

Fig. 6. Schematic illustration of the Hot Disk setup used to determine thermophysical properties mortar samples after conditioning under controlled environment

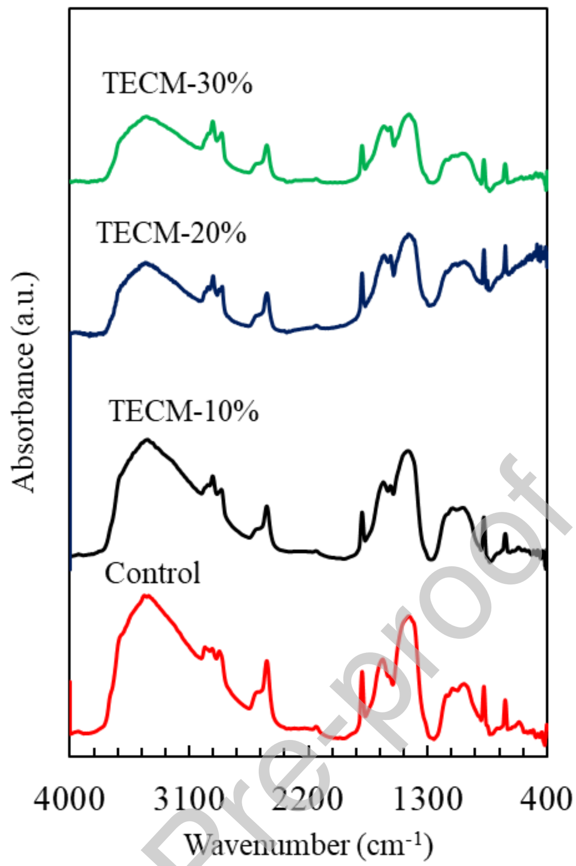

Fig. 7: FTIR spectra with and without AC_{cs}/EPCM incorporated cement mortar samples

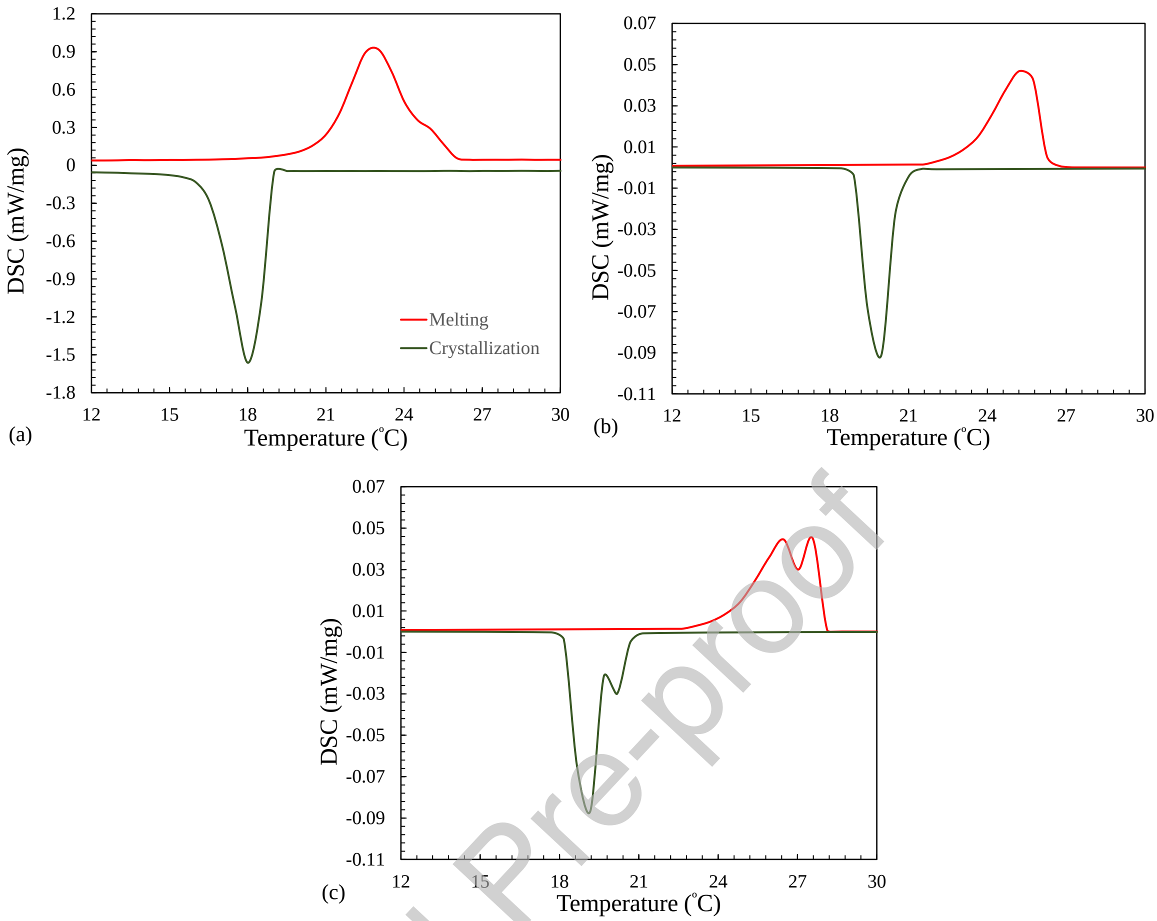

Fig. 8. DSC results of selected materials (a) EPCM; (b) AC_{cs}/EPCM; (c) AC_{cs}/EPC (1000th cycle)

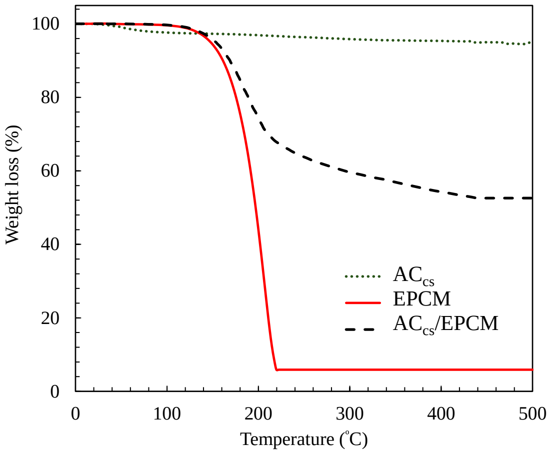

Fig. 9. TGA analysis results of AC_{cs}, EPCM and AC_{cs}/EPCM

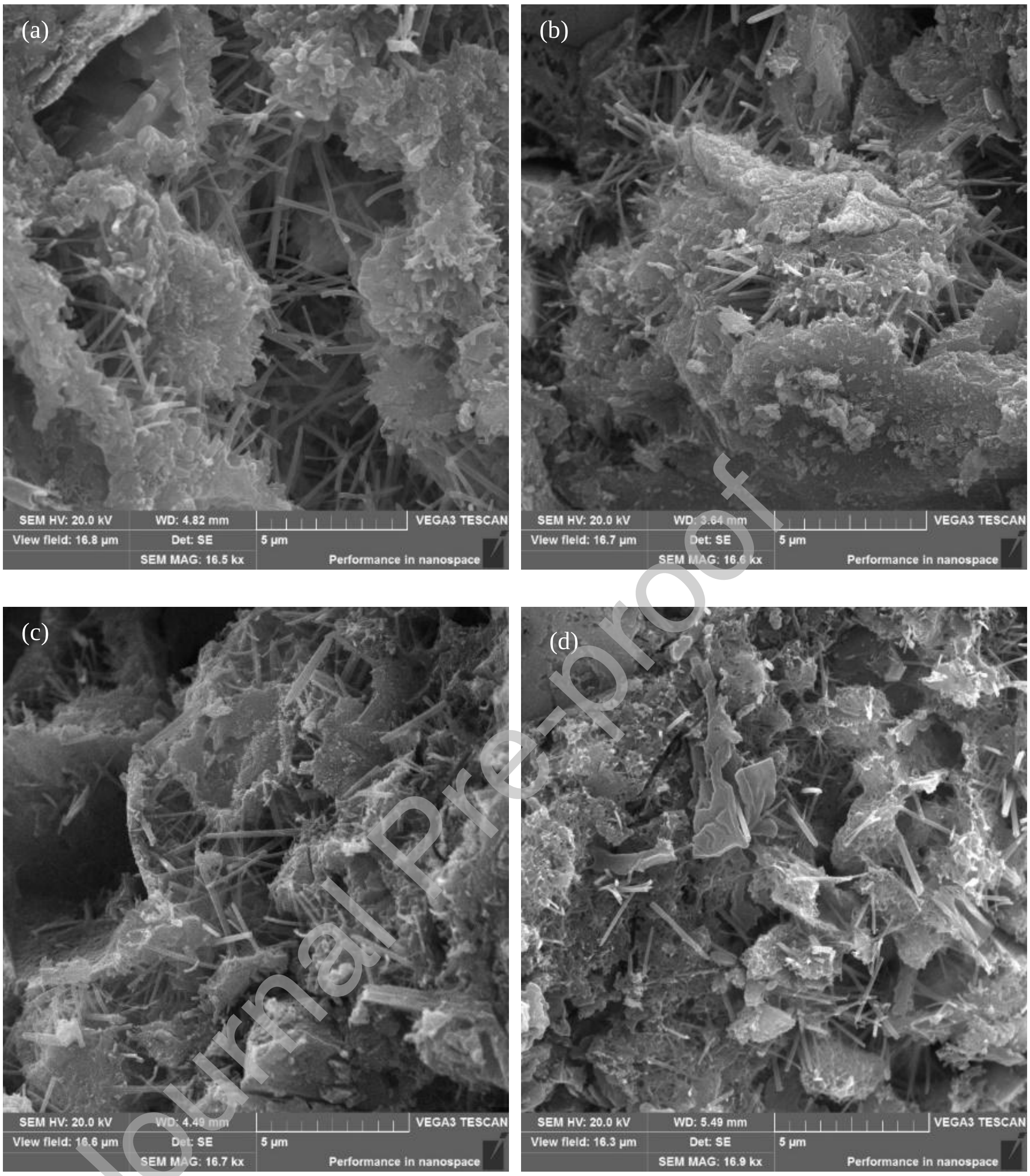

Fig. 10. SEM images of AC_{cs}/EPCM incorporated mortar samples (a) Control; (b) TECM-10%; (c) TECM-20%; (d) TECM-30%

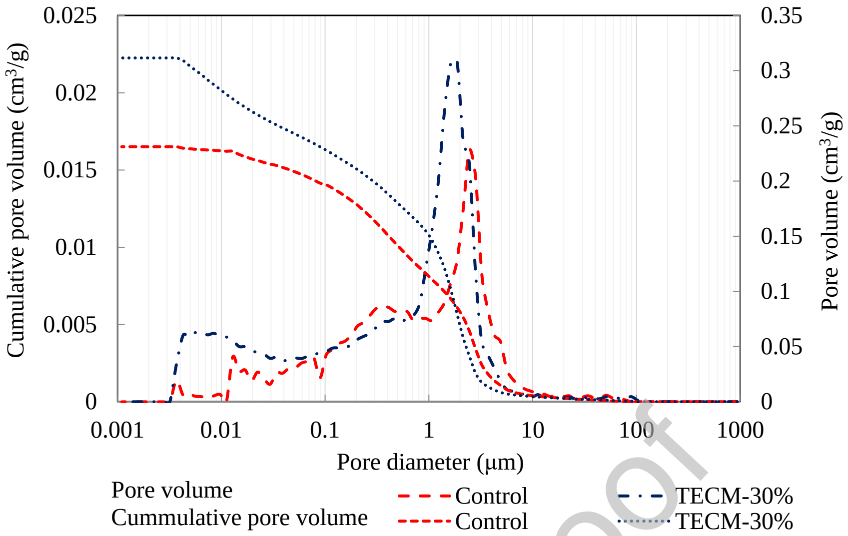

Fig. 11. Pore volume analysis of control and TECM

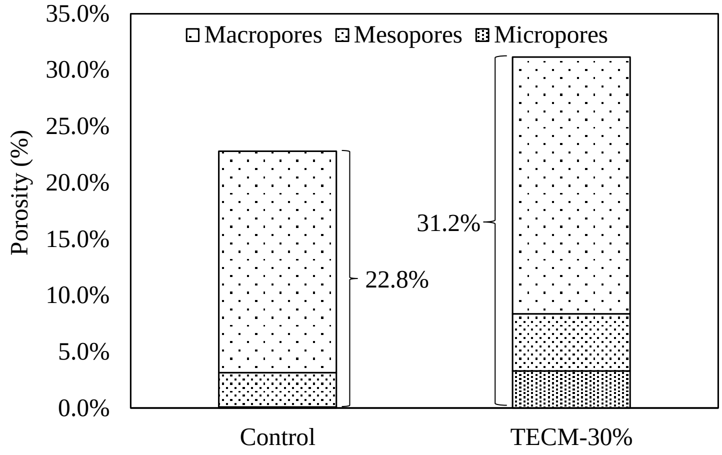

Fig. 12. Pore development analysis of control and TECM

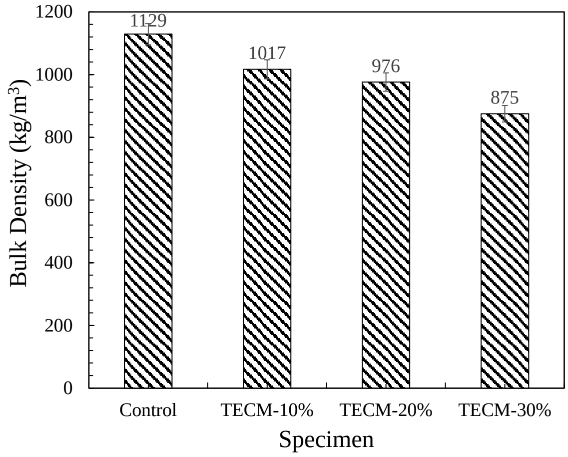

Fig. 13. Bulk density of mortar samples with/without composite PCM

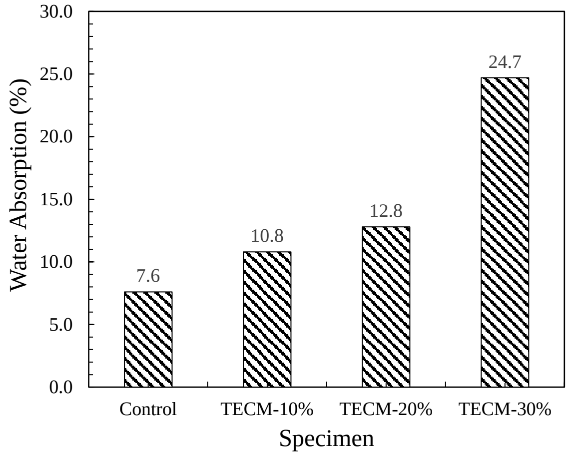

Fig. 14. Water adsorption of the control and TECM samples

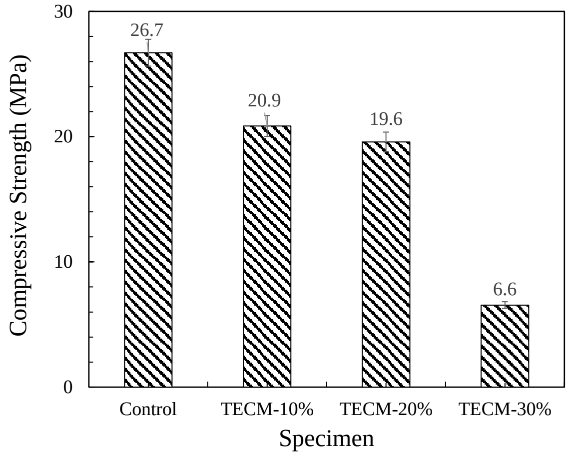

Fig. 15. Compressive strength after 28 days of the control and TECM samples

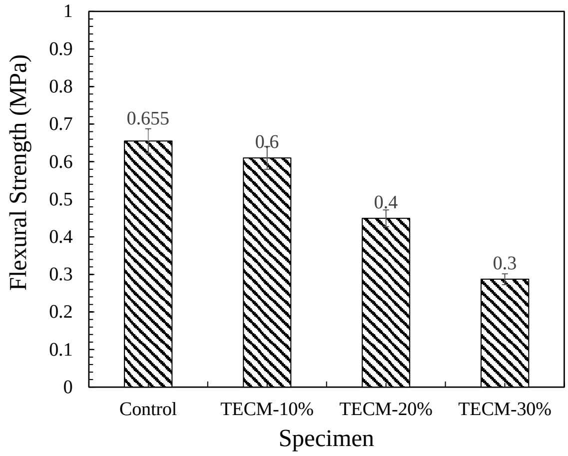

Fig. 16. Flexural strength after 28 days of the control and TECM samples

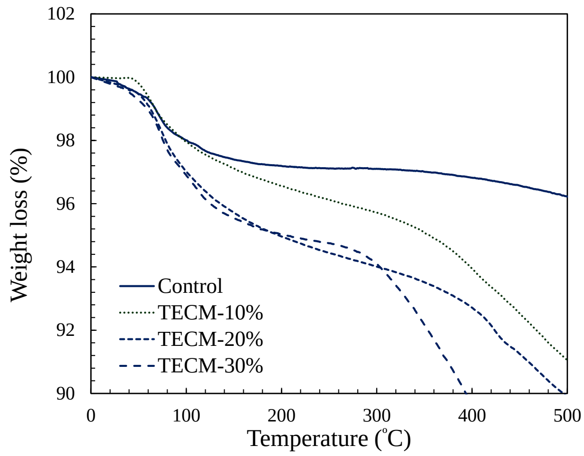

Fig. 17. TGA results of the control and TECM samples

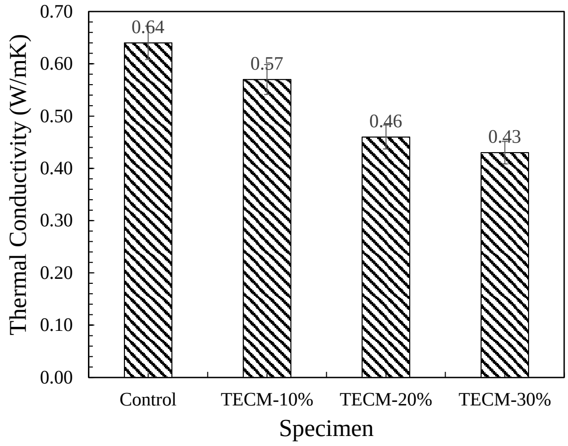

(a)

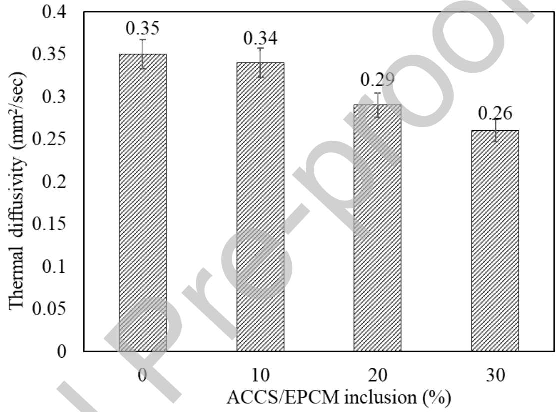

(b)

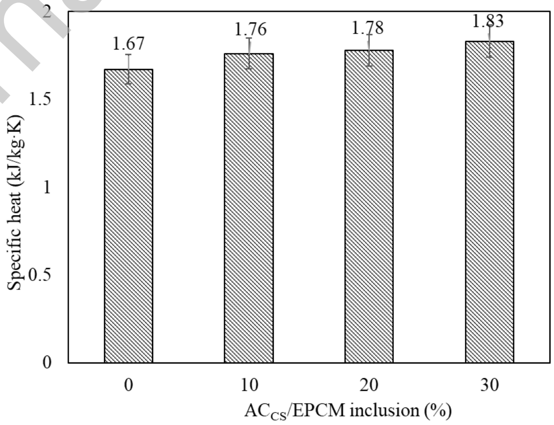

(c)

Fig. 18. Thermophysical properties of mortar samples with and without AC_{cs}/EPCM (a) thermal conductivity; (b) thermal diffusivity; (c) specific heat capacity

Table 1: Physical and mechanical properties of the cement

Property	Unit of Measurement	Average Value	Limits (EN 197/1)
Compressive Strength (24 h)	MPa	14	-
Compressive Strength (2 days)	MPa	24	≥ 20
Compressive Strength (7 days)	MPa	35	-
Compressive Strength (28 days)	MPa	49	≥ 42.5 / ≤ 62.5
Initial Setting Time	minutes	170	≥ 75
Final Setting Time	minutes	220	-
Stability	mm	0	≤ 10
Residue on 90-micron sieve	%	-	-
Residue on 63-micron sieve	%	1.2	-
Residue on 32-micron sieve	%	-	-
Specific Surface Area (Blaine)	cm^2/g	4700	-
Absolute Density	g/cm^3	2.8	-
Apparent Density	g/cm^3	1.1	-
Loss on Ignition	%	n.d.*	-
Insoluble Residue	%	n.d.*	-
SO_3 Content	%	2.5	≤ 4.0
Chlorides	%	0.04	≤ 0.10

*not detected

Table 2: Chemical composition

Parameter	SiO_2	Al_2O_3	Fe_2O_3	CaO	MgO	SO_3	Na_2O	K_2O	TiO_2	MnO
Values (%)	29.1	9.8	2.2	45.0	4.1	2.7	0.7	2.3	0.4	0.1

Table 3: Mixture proportions

Material	Cement (g)	Sand (g)	Water (g)	AC_{cs}/EPCM composite (g)
Control	450	450	337.5	0
TECM-10%	450	405	337.5	45
TECM-20%	450	360	337.5	90
TECM-30%	450	315	337.5	135

Table 4: DSC results of EPCM and AC_{cs}/EPCM

Sample	**Melting point (°C)**	ΔH_M **(J/g)**	**Crystallization point (°C)**	ΔH_C **(J/g)**
EPCM	20.5	157.2	19.0	156.3
AC_{cs}/EPCM	21.8	32.5	19.1	32.6
AC_{cs}/EPCM (1000th cycle)	22.3	31.2	21.2	31.2

Table 5. Comparison of composite PCMs incorporated mortars.

Precursor material	**Type of PCM**	**Max dosage ratio (%)**	**Thermal conductivity (W/mK)**	**Compressive strength at 28th day (MPa)**	**Ref.**
Perlite	paraffin	80	1.04	18	[94]
Diatomite	octadecane	30	0.71	18.3	[95]
Perlite	paraffin	20	0.52	13.2	[96]
Expanded graphite	n-octadecane	2.5	1.85	10.5*	[97]
Coal gasification slag	paraffin	22	1.30	18.56	[98]
Expanded graphite	paraffin	20	0.81	5.1	[99]
AC	CA-SA	25	0.41	4.78	[100]
Coconut shell based AC	CA-MA	30	0.43	6.6	This study

*curing unknown

Declaration of interests

☒ The authors declare that they have no known competing financial interests or personal relationships that could have appeared to influence the work reported in this paper.

☐ The authors declare the following financial interests/personal relationships which may be considered as potential competing interests: